

AD-A241 603



MISCELLANEOUS PAPER CERC-91-11

2

US Army Corps
of Engineers

PARAMETRIC DESCRIPTION FOR A WAVE ENERGY SPECTRUM IN THE SURF ZONE

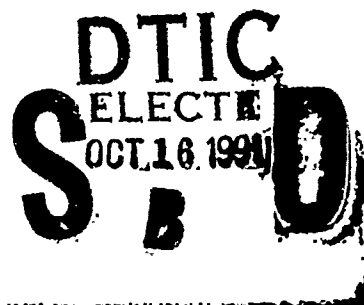
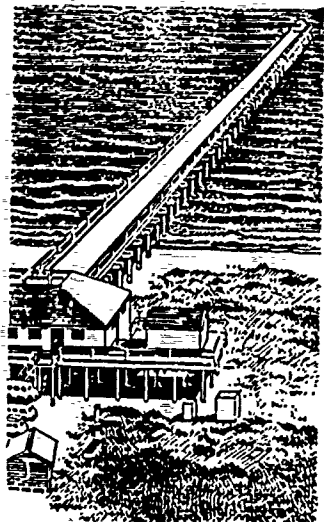
by

Jack E. Davis, Jane M. Smith, C. Linwood Vincent

Coastal Engineering Research Center

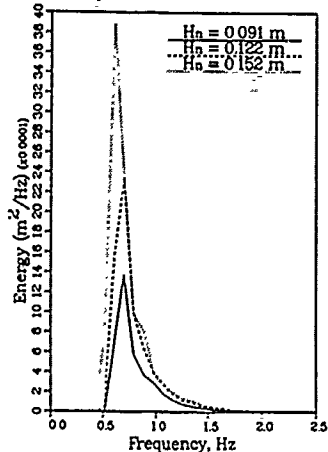
DEPARTMENT OF THE ARMY

Waterways Experiment Station, Corps of Engineers
3909 Halls Ferry Road, Vicksburg, Mississippi 39180-6199



$T_p = 1.5$

Depth = 0460



September 1991

Final Report

Approved For Public Release; Distribution Unlimited

91-13216



Prepared for DEPARTMENT OF THE ARMY
US Army Corps of Engineers
Washington, DC 20314-1000

Under Work Unit 31672



**Destroy this report when no longer needed. Do not return
it to the originator.**

**The findings in this report are not to be construed as an official
Department of the Army position unless so designated
by other authorized documents.**

**The contents of this report are not to be used for
advertising, publication, or promotional purposes.
Citation of trade names does not constitute an
official endorsement or approval of the use of
such commercial products.**

REPORT DOCUMENTATION PAGE			Form Approved OMB No. 0704-0188	
<small>Public reporting burden for this collection of information is estimated to average 1 hour per response, including the time for reviewing instructions, searching existing data sources, gathering and maintaining the data needed, and completing and reviewing the collection of information. Send comments regarding this burden estimate or any other aspect of this collection of information, including suggestions for reducing this burden to Washington Headquarters Services, Directorate for Information Operations and Reports, 1215 Jefferson Davis Highway, Suite 1204, Arlington, VA 22202-4302, and to the Office of Management and Budget, Paperwork Reduction Project (0704-0188), Washington, DC 20503.</small>				
1. AGENCY USE ONLY (Leave blank)	2. REPORT DATE September 1991	3. REPORT TYPE AND DATES COVERED Final report		
4. TITLE AND SUBTITLE Parametric Description for a Wave Energy Spectrum in the Surf Zone		5. FUNDING NUMBERS Work Unit 31672		
6. AUTHOR(S) Jack E. Davis, Jane M. Smith, C. Linwood Vincent				
7. PERFORMING ORGANIZATION NAME(S) AND ADDRESS(ES) USAE Waterways Experiment Station, Coastal Engineering Research Center, 3909 Halls Ferry Road, Vicksburg, MS 39180-6199		8. PERFORMING ORGANIZATION REPORT NUMBER Miscellaneous Paper CERC-91-11		
9. SPONSORING/MONITORING AGENCY NAME(S) AND ADDRESS(ES) US Army Corps of Engineers Washington, DC 20314-1000		10. SPONSORING/MONITORING AGENCY REPORT NUMBER		
11. SUPPLEMENTARY NOTES Available from National Technical Information Service, 5285 Port Royal Road, Springfield, VA 22161				
12a. DISTRIBUTION / AVAILABILITY STATEMENT Approved for public release; distribution unlimited		12b. DISTRIBUTION CODE		
13. ABSTRACT (Maximum 200 words) The work described in this report characterizes the shoaling and breaking processes of wave-energy spectra by describing their limiting form in the surf zone. The Field Research Facility spectral description was fit to laboratory spectra, and linear regressions were performed to determine functional relationships between the spectral parameters and environment variables such as peak spectral period (wavelength), total spectral energy, and water depth. The spectral representation for shoaling and breaking spectra was coded in a numerical spectral wave model that was used to simulate the laboratory data. The model and laboratory results were compared. While the simulation did not verify the spectral representation, it did indicate the feasibility of the approach.				
14. SUBJECT TERMS See reverse.			15. NUMBER OF PAGES 47	
			16. PRICE CODE	
17. SECURITY CLASSIFICATION OF REPORT UNCLASSIFIED	18. SECURITY CLASSIFICATION OF THIS PAGE UNCLASSIFIED	19. SECURITY CLASSIFICATION OF ABSTRACT	20. LIMITATION OF ABSTRACT	

14. SUBJECT TERMS (Continued).

Laboratory experiments
Numerical modeling
Spectral wave modeling
Spectral wave transformations
STWAVE model
Surf zone processes
Wave breaking
Wave energy spectra
Wave shoaling
Wave transformations

PREFACE

This study was authorized by the Headquarters, US Army Corps of Engineers (HQUSACE), under the Coastal Flooding and Storm Protection Program, Work Unit 31672, "Nearshore Waves and Currents." The research was conducted by the Coastal Engineering Research Center (CERC) of the US Army Engineer Waterways Experiment Station (WES). The Technical Monitors were Messrs. John H. Lockhart, Jr.; John G. Housley; James E. Crews; and Robert H. Campbell. Dr. C. Linwood Vincent of CERC was the Program Manager.

This report was prepared by Mr. Jack E. Davis, Coastal Oceanography Branch (COB), Research Division (RD), CERC. Portions of the introduction were prepared by Dr. Vincent, and the description of the laboratory setup was provided by Ms. Jane M. Smith, COB. The work was performed under the direct supervision of Dr. Martin C. Miller, Chief, COB, and Mr. H. Lee Butler, Chief, RD, and under the general supervision of Mr. Charles C. Calhoun, Jr., Assistant Chief, CERC, and Dr. James R. Houston, Chief, CERC.

The Commander and Director of WES during preparation of this report was COL Larry B. Fulton, EN. The Technical Director of WES was Dr. Robert W. Whalin.

Accession For	
NTIS GRA&I	<input checked="checked" type="checkbox"/>
DTIC TAB	<input type="checkbox"/>
Unannounced	<input type="checkbox"/>
Justification	
By _____	
Distribution/	
Availability Codes	
Dist	Avail and/or Special
A-1	

CONTENTS

	<u>Page</u>
PREFACE	1
PART I: BACKGROUND	3
PART II: LABORATORY STUDY	7
Physical Facility	7
Laboratory Spectra	7
PART III: ANALYSIS	10
Preparation of Data	10
Fitting Calculated To Measured Spectra	10
Linear Regression for FRF Parameters	16
PART IV: APPLICATION IN SPECTRAL MODEL	27
PART V: SUMMARY AND CONCLUSIONS	38
REFERENCES	39
APPENDIX A: WAVE CHARACTERISTIC AND FIELD RESEARCH FACILITY SPECTRAL PARAMETER VALUES	A1

PARAMETRIC DESCRIPTION FOR A WAVE ENERGY SPECTRUM
IN THE SURF ZONE

PART I: BACKGROUND

1. Coastal processes, such as currents, water setup, sediment transport, and forces on structures, depend strongly on the nature of breaking waves nearshore. Though the theory for modeling breaking waves is incomplete, a few practical procedures have been advanced that provide estimates of wave heights in the nearshore for engineering purposes. A large body of literature exists on the breaking characteristics of regular waves (Shore Protection Manual (SPM) 1984). Substantial progress has been made in recent years toward representing irregular wave breaking by modifying the probability distribution of wave heights within the surf zone to account for broken waves (e.g. Battjes 1972). Progress has also been made toward representing the irregular waves by a wave-energy spectrum derived from a Fourier transform of the sea surface. In spectral descriptions for waves, breaking has often been represented by limiting the spectrum to a deterministic shape or to given equilibrium range power laws (e.g., Kitaigorodskii 1983 and Bouws et al. 1985).

2. The work described herein is an attempt to characterize the shoaling and breaking processes of a wave-energy spectrum by describing its limiting form in the surf zone. Observations of laboratory data suggested that energy spectra converged to a consistent shape for given peak periods regardless of the total deepwater energy. More rigorous study of the laboratory data was intended to determine whether a wave-energy spectrum would therefore attain a characteristic shape in the region of breaking which may be described by an analytical function, and whether the parameters of that spectral function correlated with relevant physical parameters of the waves (or spectrum) and bathymetry.

3. A one-dimensional flume designed to investigate wave shoaling without refraction was used to study the propagation characteristics of a variety of wave spectra. The spectra would represent wind-sea or energetic swell, if scaled to prototype dimensions. During the investigation, two significant features of the propagating spectra were noted. First, the generation of a high-frequency peak at a harmonic of the main peak of the spectrum was

evident, indicating the presence of nonlinear interactions between frequencies as the spectra shoaled. Such nonlinear interactions occurring during shoaling were neglected during this investigation since they could not be represented by the linear spectral theory. Figure 1 shows examples of defined high-frequency harmonic peaks developed as the spectra shoaled. Each spectrum shown in Figure 1 had the same initial peak period ($T_p = 2.0$ sec), though different initial total spectral energies.

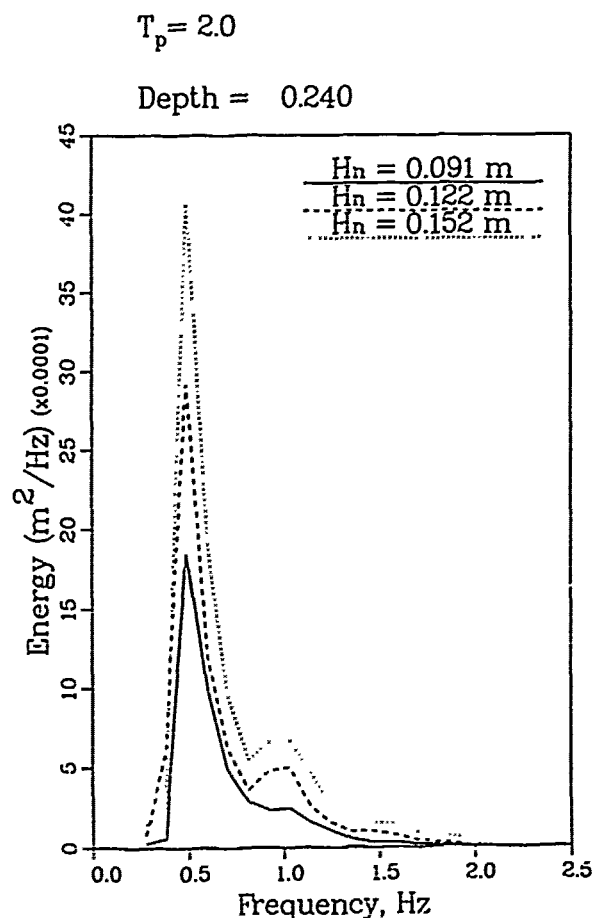
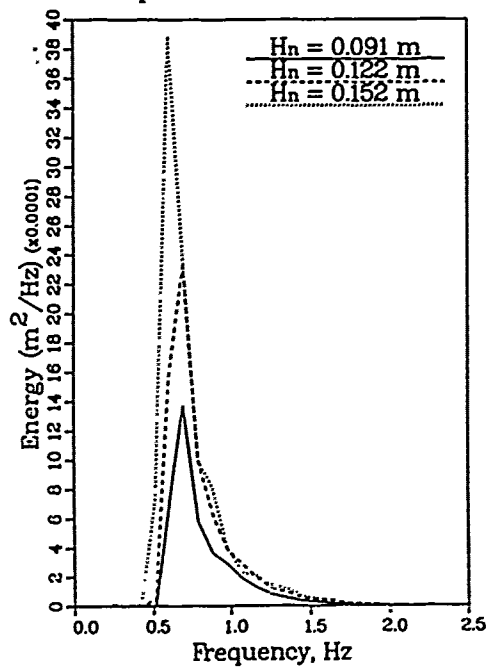


Figure 1. Example of clearly defined high-frequency harmonics

4. The second feature noted in the laboratory data was the tendency of the spectra to conform after breaking to a constant spectral shape and size for a given peak spectral period irrespective of the level of energy in the initial spectrum. Figure 2 shows an example of three spectra that had the same peak spectral period, but different initial energies, both before and after breaking. The spectra clearly conform to a similar shape and size once

$$T_p = 1.5$$

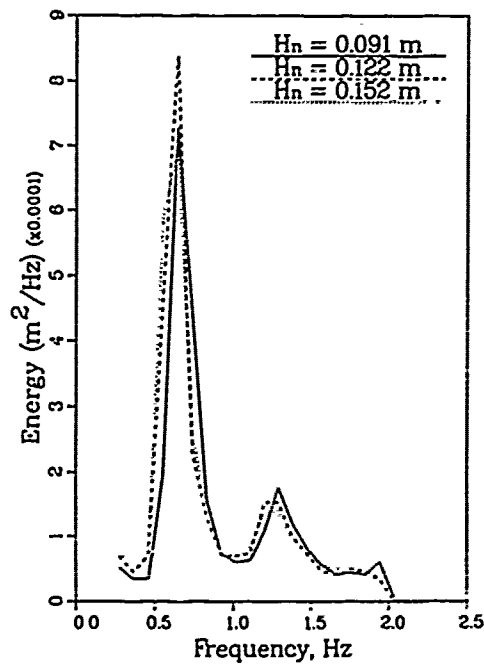
$$\text{Depth} = 0.460$$



a. In deep water

$$T_p = 1.5$$

$$\text{Depth} = 0.090$$



b. After breaking

Figure 2. Comparisons of spectra in deepwater and after breaking indicate conforming spectral shapes

they have entered the surf zone. The recognition of the phenomenon that breaking spectra conform to a constant shape and size supported the expectation that the surf-zone spectra could be described mathematically. It was anticipated that the parameter values in existing spectral descriptions, such as the TMA spectrum (Bouws et al. 1985), named after the experiments Trexel, Marsten, and Arsloe used to describe the spectrum, or the FRF spectrum (Miller and Vincent 1990), named after the location at which spectral data were collected, might be constants or related directly to the wave characteristics or water depths.

5. The approach taken in this study is described briefly below:

- a. The laboratory spectra were evaluated to determine which spectra clearly broke during propagation.
- b. TMA and FRF spectral descriptions were fit to each of the measured spectra by iterating on the values of the respective spectral parameters until a best fit was achieved. (During this process of fitting computed spectra to measured spectra, it was noted that the TMA spectrum did not fit the measured spectra well near the surf zone, even though the laboratory spectra were generated with a TMA spectral shape. Therefore, analysis of the TMA spectral parameters was omitted.)
- c. The values of the FRF spectral parameters, found for each of the measured spectra, were linearly regressed against non-dimensional formulations of the local and deepwater spectral wave characteristics in order to determine functional descriptions for the parameters.
- d. The accuracy of the FRF spectral parameter formulation for describing the laboratory spectra was checked by implementing the formulation in the time-independent spectral wave model, STWAVE. The model was used to simulate the laboratory spectra. Then the simulated and measured spectra were compared.

6. The following sections describe the analysis of the laboratory spectra, including a description of the laboratory setup and experiments, the spectral fitting and regression procedures, and the final implementation of the regression results in STWAVE.

PART II: LABORATORY STUDY

Physical Facility

7. The laboratory wave spectra were generated by a piston-type paddle in a 0.46-m-wide, 45.7-m-long, and 0.9-m-deep wave flume (Figure 3). The depth in the flume was constant (0.61 m) from the wave paddle to the middle of the flume, from which point the bottom rose on a constant slope of 0.0333. The flume had a smooth concrete bottom and clear Plexiglas walls. Eight electrical resistance gages were used to measure the variation of the water surface. One of these gages marked the toe of the slope where the water depth was 0.61 m. The other gages were placed in the sloping section at depths of 0.46, 0.30, 0.24, 0.18, 0.12, 0.09, and 0.06 m.

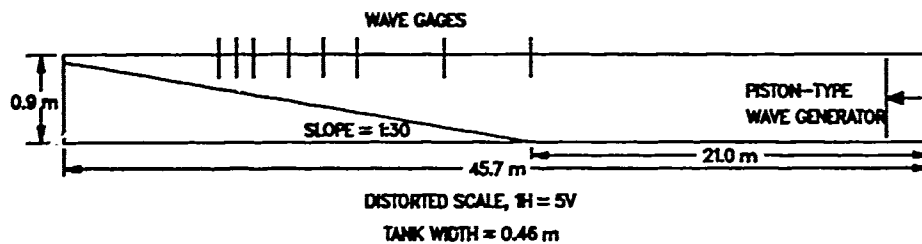


Figure 3. Schematic of the laboratory flume

Laboratory Spectra

8. Thirty different wave-energy spectra were generated in the flume combining six different peak spectral periods (1.25, 1.5, 1.75, 2.0, 2.25 and 2.5 sec) with five different energy-based wave heights (0.03, 0.06, 0.09, 0.12, and 0.15 m). Each spectrum was generated with the TMA (Bouws et al. 1985) spectral shape given by:

$$E_{TMA}(f) = E_p(\alpha, f) \phi_{pc}\left(\frac{f}{f_p}\right) \phi_j(f, f_p, \gamma, \sigma_a, \sigma_b) \phi(2\pi f, h) \quad (1)$$

where

E_{TMA} = spectral energy for the frequency, f

f = spectral frequency

α = Phillips' equilibrium constant

f_m = frequency containing the peak spectral energy

γ = spectral peakedness factor

σ_a = spectral width factor below the peak spectral frequency

σ_b = spectral width factor above the peak spectral frequency

h = water depth

The factors E_p , ϕ_{p2} , ϕ_j , and ϕ are given by:

$$E_p(\alpha, f) = \frac{\alpha g^2}{2\pi} f^{-5} \quad (2)$$

$$\phi_{p2}\left(\frac{f}{f_m}\right) = \exp\left[-1.25\left(\frac{f}{f_m}\right)^{-4}\right] \quad (3)$$

$$\phi_j(f, f_m, \gamma, \sigma_a, \sigma_b) = \gamma \exp\left[\frac{-(f-f_m)^2}{(2\sigma^2 f_m^2)}\right] \quad (4)$$

$$\phi(2\pi f, h) = [R(\omega_h)]^{-2} \left\{ 1 + \frac{2\omega_h^2 R(\omega_h)}{\sinh[2\omega_h^2 R(\omega_h)]} \right\}^{-1} \quad (5)$$

where

g = gravitational acceleration

$\sigma = \sigma_a$ for $f < f_m$,

σ_b for $f \geq f_m$

and

$$\omega_h = 2\pi f \left(\frac{h}{g}\right)^{\frac{1}{2}} \quad (6)$$

$R(\omega_h)$ was found by approximating the solution to $R(\omega_h) \tanh[\omega_h^2 R(\omega_h)] = 1$.

The spectral parameter values used to generate the laboratory spectra were

$\gamma = 3.3$, $\sigma_a = 0.07$, and $\sigma_b = 0.09$. The values of f_m corresponded with

the inverse of the peak spectral periods listed, while the values of α were adjusted such that the total energies within the spectra were related to the desired wave heights listed.

PART III: ANALYSIS

Preparation of Data

9. The spectra derived from the time series of the water surface using Fourier transformations contained 150 to 350 frequency bands per spectrum. To tighten the confidence bands on the spectra, the number of frequency bands per spectrum was reduced to 50 in all cases by averaging over the appropriate number of frequency bands. A plot of one of the spectra is presented in Figure 4 with the original and averaged spectra superimposed. The plot indicates that the averaged spectrum retained the overall structure of the original spectrum in the primary frequency range. Wave heights computed at each gage for the original and averaged spectra are plotted in Figures 5 and 6 showing that the total energy within each spectrum was negligibly affected by the averaging.

10. Since the primary goal of this research was to determine descriptions for spectra within the surf zone, a determination was made as to which spectra broke during the laboratory tests. Only spectra associated with wave heights greater than 0.09 m broke during these tests, reducing the number of tests from 30 to 18. Therefore, a total of 144 (18 tests \times 8 gages) measured spectra were used in the initial analysis.

Fitting Calculated to Measured Spectra

11. The measured spectra were "fit" by the FRF spectral description (Miller and Vincent 1990). In the present context, the word "fit" implies that the FRF spectral parameters were adjusted until the calculated spectrum closely approximated the measured spectrum. The closeness of fit was determined by visual inspection. The form of the FRF spectrum used was expressed as

$$E_{FRF}(f) = S(\omega, \beta, h, \alpha_o) \phi_{pm}\left(\frac{f}{f_m}\right) \phi_j(f, f_m, \gamma, \sigma_a, \sigma_b) \quad (7)$$

where S is

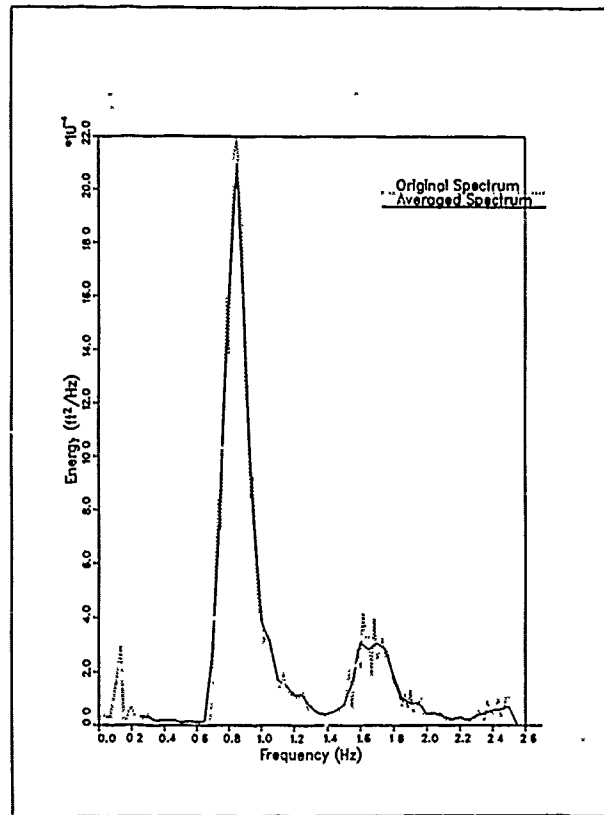


Figure 4. Original and averaged spectrum*

$$S(\omega, \beta, h, \alpha_o) = \frac{\alpha_o g^{-\frac{1}{2}} \beta k^{-2.5}}{\frac{\delta \omega}{\delta k} | \omega^2 = gk \tanh(kh) } \quad (8)$$

and

ω = angular frequency (= $2\pi f$)

β = wind speed at the 10-m elevation

α_o = equilibrium range constant (= 0.0029)

12. In Equation 7, the value of β controls the energy level within the high-frequency portion of the spectrum; γ is the peakedness parameter; σ_a controls the width of the spectral peak to the low-frequency side, and σ_b controls the width of the spectral peak to the high-frequency side. In application of the FRF spectrum to prototype conditions, the dimensional parameter β (length/time) is equivalent to the 10-m elevation wind speed and is

* To convert square feet into square meters, multiply by 0.09290304.

FRF Spectral Parameter Analysis Surf-Zone Breaking

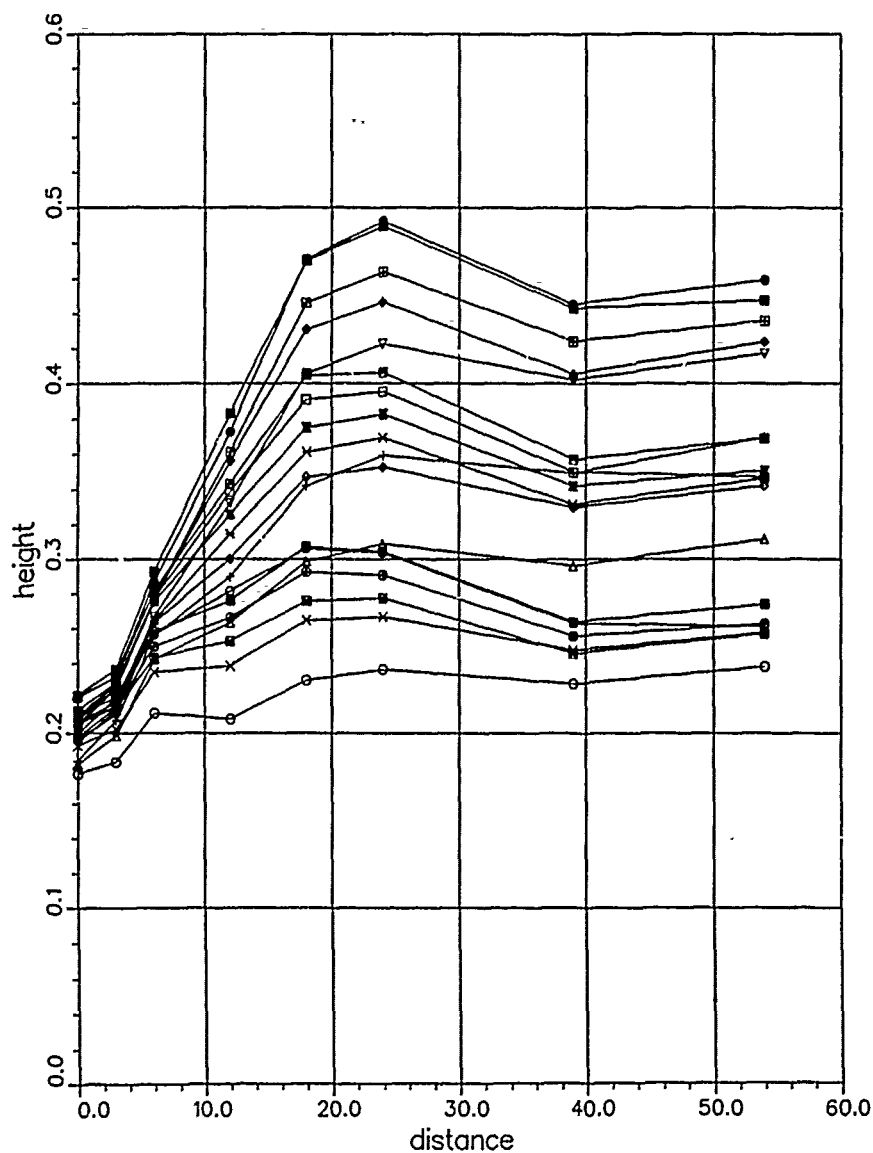


Figure 5. Energy-based wave height computed from the original laboratory (each line represents a different test)

FRF Spectral Parameter Analysis Surf-Zone Breaking

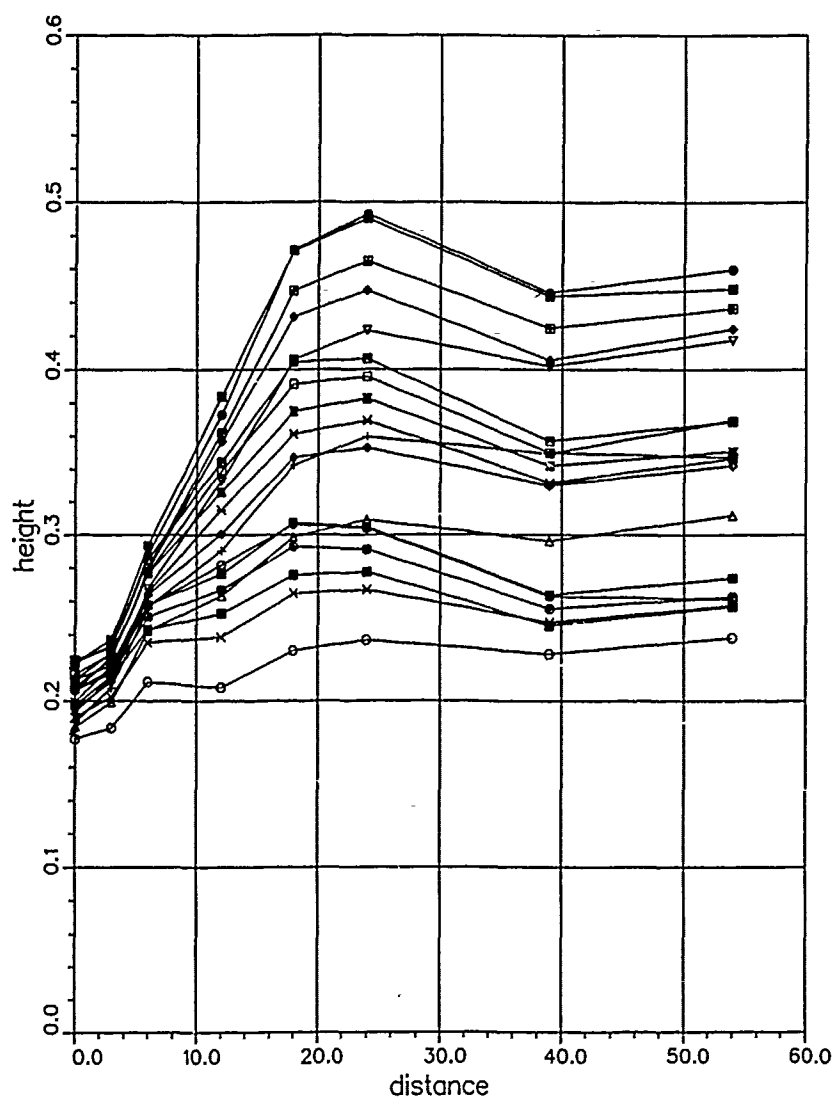


Figure 6. Energy-based wave height computed from the averaged spectra (each line represents a different test)

obtained from local meteorological data. In the laboratory experiments, however, the wave spectra were generated by a wave paddle and not the wind. Under such conditions, β acts like a spectral parameter, reminiscent of α in Equation 1, more than it represents a wind speed. Further, when one considers the surf zone in either prototype or laboratory setups, β is independent of the wind speed, as will be shown. (Note that Miller and Vincent (1990), who studied prototype wave energy spectra outside the surf zone, replaced β with U_{10} to clearly identify it as related to wind speed.)

13. Values of the parameters β , γ , σ_a , and σ_b found to be the best fit to the measured spectra are provided in Table A1 (Appendix A). In Table A1, lengths are in meters, h is the water depth at the particular gage, and T_n and H_n are the nominal periods and wave heights from which the laboratory spectra were generated, although the actual spectra generated usually had periods and wave heights different from T_n and H_n . The value of H_{mo} is the local energy-based wave height given by:

$$H_{mo} = 4 \sqrt{\int E_{FRF}(f) df} \quad (9)$$

The value of L is the local wavelength approximated by:

$$L = L_o \sqrt{\tanh\left(\frac{2\pi h}{L_o}\right)} \quad (10)$$

where the deepwater wavelength L_o is given by:

$$L_o = \frac{g}{2\pi} T_p^2 \quad (11)$$

and

T_p = peak spectral period ($= 1/f_m$).

The value of H_o was equal to H_{mo} at the deepest gage (Gage 8).

14. During the preliminary regression analysis, it was noted that the data at Gage 1 (the shallowest gage) may have been measured improperly. The water surface elevation measurements may have been adversely affected by the shallow water, wave runup, surf beat, etc. The wave heights (Figures 5 and 6) did not approach zero as the waves moved toward the beach; instead, the slope of the wave heights between Gages 1 and 2 decreased. Due to this unexpected behavior, the final regression analysis excluded the data (18 spectra) from

Gage 1. Also, during the preliminary regression analysis, it was noted that the TMA spectral shape generated at the wave paddle maintained its shape through Gages 7 and 8. Hence, satisfactory fits between the calculated FRF spectra and the measured spectra at these gages were not possible due to the difference in the high-frequency energy representation of the TMA and FRF spectra, where the former is of an f^5 and the latter is of an f^4 type (Figure 7). Since the measured spectra at Gages 7 and 8 could not be matched properly, these data (36 spectra) were also excluded from the final regression analysis. The final regression analysis was therefore based on the remaining 90 measured spectra from Gages 2 to 6.

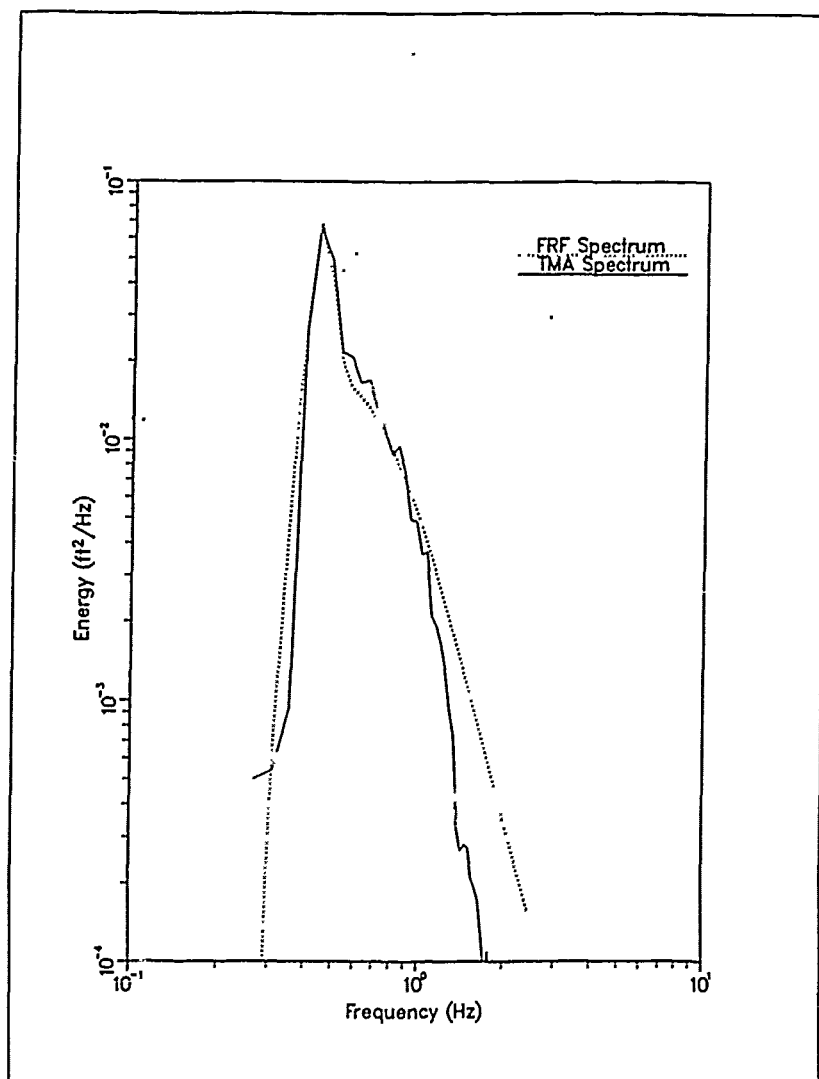


Figure 7. Example of the difference between the equilibrium range slopes for a TMA and an FRF spectrum

Linear Regression for FRF Parameters

Equation formulation

15. The parameters γ , σ_a , σ_b and a nondimensional form of β (β/C , where C is the wave celerity given by $C = L/T_p$) were linearly regressed against nondimensional formulations of the local and deepwater wave characteristics (H_{mo} , H_o , L , and h). The regressions were based on the linear equation:

$$\log(Y) = b + a_1 \log(X_1) + a_2 \log(X_2) \quad (12)$$

where

Y = spectral parameter to regress, i.e., γ , σ_a , or σ_b and β/C

X_1 = first regression parameter, i.e., h/L or h/L_o

X_2 = second regression parameter, i.e., H/h or H_o/h

b = regression constant

a_1 = coefficient for first regression parameter

a_2 = coefficient for second regression parameter

Once the regression constants and coefficients in Equation 12 were determined, the inverse logarithms of both sides of Equation 12 were taken to yield:

$$Y = \log^{-1}(b) X_1^{a_1} X_2^{a_2} \quad (13)$$

16. Initially, X_1 and X_2 were equated respectively to h/L and H_{mo}/h to determine the relationship of Y (β , γ , σ_a , or σ_b) with local wave characteristics. X_1 and X_2 were then equated respectively to h/L_o and H_o/h to determine the relationship of Y with the deepwater wave characteristics. It is worthwhile to note that, for a given regression, the regressors mentioned above can be rearranged to form other wave parameter ratios. For example, the equation:

$$\gamma = \log^{-1}(b) \left(\frac{h}{L}\right)^{a_1} \left(\frac{H}{h}\right)^{a_2} \quad (14)$$

can be rearranged to an equivalent expression where the influence of wave steepness (H/L) can be evaluated, i.e.:

$$\gamma = \log^{-1}(b) \left(\frac{h}{L}\right)^{(-a_2 + a_1)} \left(\frac{H}{L}\right)^{a_2} \quad (15)$$

17. Table 1 provides results of the regression analysis for β/C and γ based on the deepwater and local wave characteristics. The table contains the regression constant and coefficients (b , a_1 , and a_2) for each regression, along with standard errors in those values, the related correlation coefficient, and the r^2 value.

Regression for β/C

18. The regression analysis showed a strong correlation between β/C and the local wave characteristics as shown in Figure 8. β/C was also strongly correlated with the deepwater wave characteristics as shown in Figure 9. The regression equations found for β/C are:

$$\frac{\beta}{C} = 25.1 \left(\frac{h}{L} \right)^{0.48} \left(\frac{H}{h} \right)^{1.9} \quad (16)$$

when based on the local wave characteristics and

$$\frac{\beta}{C} = 4.47 \left(\frac{h}{L_o} \right)^{0.08} \left(\frac{H_o}{h} \right)^{0.99} \quad (17)$$

when based on the deepwater wave characteristics. Recognizing that the influence of h/L_o in Equation 17 is small due to the small exponent on the ratio, a regression was performed based solely on H_o/h . While the regression constant b and the coefficient a_2 were modified when h/L_o was removed from the regression, the correlation coefficient remained unchanged (Table 1). The results of the regression are plotted in Figure 10. The resulting regression equation is:

$$\frac{\beta}{C} = 3.24 \left(\frac{H_o}{h} \right)^{0.92} \quad (18)$$

19. Equation 18 suggests that energy in the equilibrium range of a given spectrum is directly proportional to the deepwater wave height. Hence, spectra with the same values for T_p but different values for H_o will have different amounts of energy in the equilibrium range of the spectrum when in the surf zone. This suggestion is contrary to the general observations of the spectra which indicated that the spectral energy within the surf zone was

Table 1
Regression Results

$$Y = U_{10}/C, \quad X_1 = h/L, \quad X_2 = H/h$$

$$\begin{array}{llll} r = 0.95 & r^2 = 0.91 & & \\ b = 1.40 & a_1 = 0.48 & a_2 = 1.93 & \\ \text{Std. Err. in: } b = 0.06 & a_1 = 0.07 & a_2 = 0.08 & \end{array}$$

$$Y = U_{10}/C, \quad X_1 = h/L_0, \quad X_2 = H_0/h$$

$$\begin{array}{llll} r = 0.92 & r^2 = 0.85 & & \\ b = 0.65 & a_1 = 0.08 & a_2 = 1.99 & \\ \text{Std. Err. in: } b = 0.08 & a_1 = 0.04 & a_2 = 0.06 & \end{array}$$

$$Y = U_{10}/C, \quad X_1 = H_0/h$$

$$\begin{array}{llll} r = 0.92 & r^2 = 0.85 & & \\ b = 0.51 & a_1 = 0.00 & a_2 = 0.92 & \\ \text{Std. Err. in: } b = 0.09 & a_1 = 0.04 & & \end{array}$$

$$Y = \gamma, \quad X_1 = h/L, \quad X_2 = H/h$$

$$\begin{array}{llll} r = 0.95 & r^2 = 0.91 & & \\ b = 3.00 & a_1 = 1.82 & a_2 = 0.34 & \\ \text{Std. Err. in: } b = 0.08 & a_1 = 0.09 & a_2 = 0.10 & \end{array}$$

$$Y = \gamma, \quad X_1 = h/L_0, \quad X_2 = H_0/h$$

$$\begin{array}{llll} r = 0.95 & r^2 = 0.91 & & \\ b = 2.24 & a_1 = 0.92 & a_2 = 0.17 & \\ \text{Std. Err. in: } b = 0.08 & a_1 = 0.04 & a_2 = 0.05 & \end{array}$$

$$Y = \gamma, \quad X_1 = h/L_0$$

$$\begin{array}{llll} r = 0.95 & r^2 = 0.91 & & \\ b = 2.10 & a_1 = 0.84 & a_2 = 0.00 & \\ \text{Std. Err. in: } b = 0.08 & a_1 = 0.03 & & \end{array}$$

* Std. Err. = standard error.

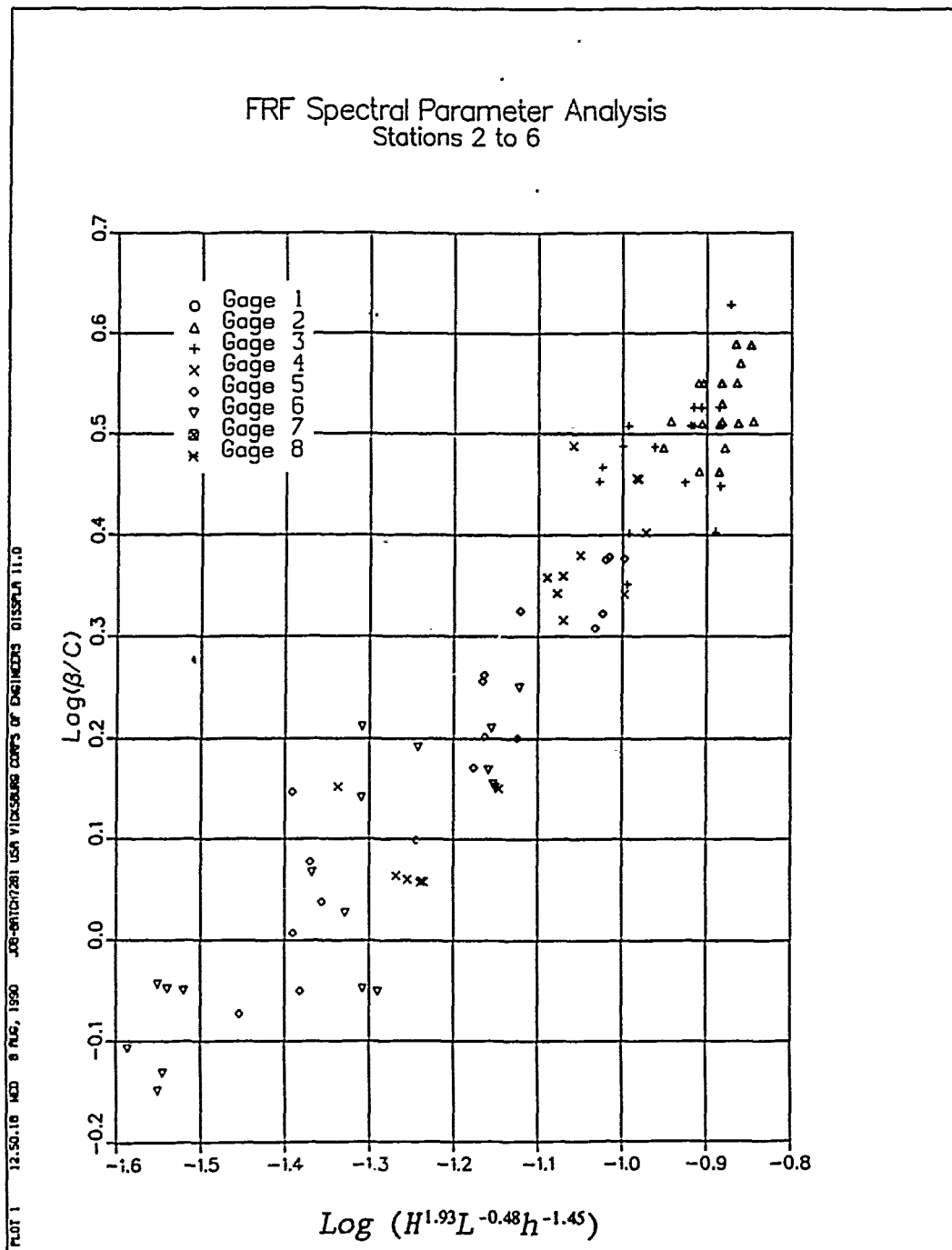


Figure 8. Regression results for β/C based on the local wave characteristics

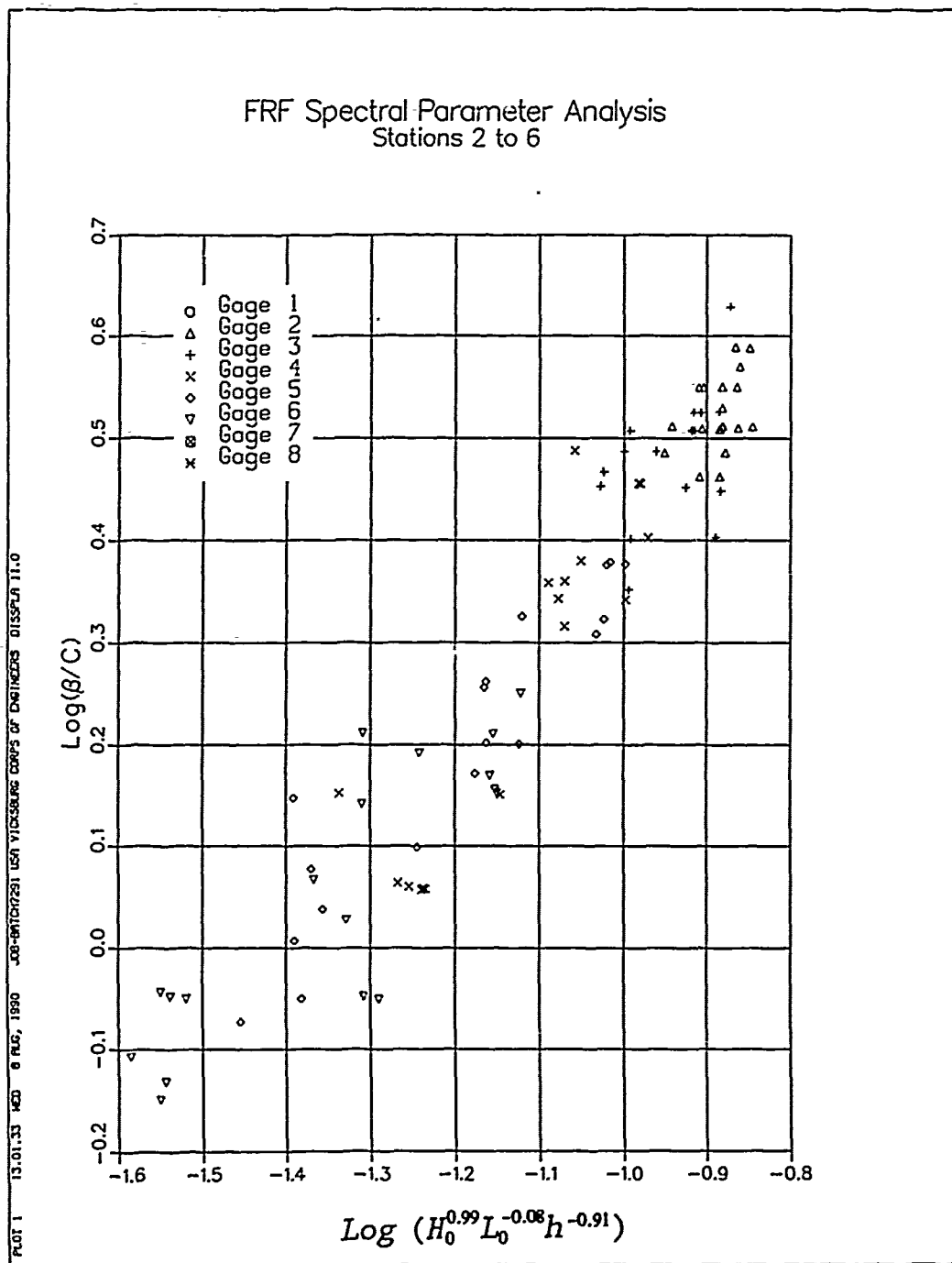


Figure 9. Regression results for β/C based on the deepwater wave results

independent of the spectral energy in deep water (Figure 2). Further inspection of the data showed that while Equation 18 was a generally good descriptor for the value of β/C seaward of the surf zone, it failed to adequately represent β/C within the surf zone. Figure 10 shows that at Gages 2 and 3 (well within the surf zone), β/C becomes independent of H_o/h . The arithmetic average of β/C from Gages 2 and 3 is 3.2 with a maximum value of 4.2 and a minimum value of 2.2. The standard deviation is 0.4, while the variance is 0.2. Hence, a value of 3.2 should be used for β/C within the surf zone.

Regression for γ

20. The regression analysis showed a strong correlation between γ and the local wave characteristics as shown in Figure 11, as well as with the deepwater wave characteristics as shown in Figure 12. The resulting regression equations are:

$$\gamma = 1000 \left(\frac{h}{L} \right)^{1.8} \left(\frac{H_o}{h} \right)^{0.34} \quad (19)$$

when based on the local wave characteristics and

$$\gamma = 174 \left(\frac{h}{L_o} \right)^{0.92} \left(\frac{H_o}{h} \right)^{0.17} \quad (20)$$

when based on the deepwater wave characteristics. Recognizing that the strength of H_o/h in Equation 20 is small, a regression was performed based solely on h/L_o . The correlation coefficient for the regression remained unchanged even though H_o/h was removed (Table 1). The results of the regression are shown in Figure 13. The resulting regression equation is

$$\gamma = 126 \left(\frac{h}{L_o} \right)^{0.84} \quad (21)$$

21. The form of Equation 21 for calculating γ is fortuitous, in that γ depends only on the deepwater wavelength which is readily available given the peak period of the spectrum of interest. Equation 21 must be applied with caution, though, since the variational characteristics of γ were based on the propagation of spectra generated with a constant γ . Additional analysis of spectra with a variety of initial γ values is needed to improve confidence in the expression for γ .

FRF Spectral Parameter Analysis Stations 2 to 6

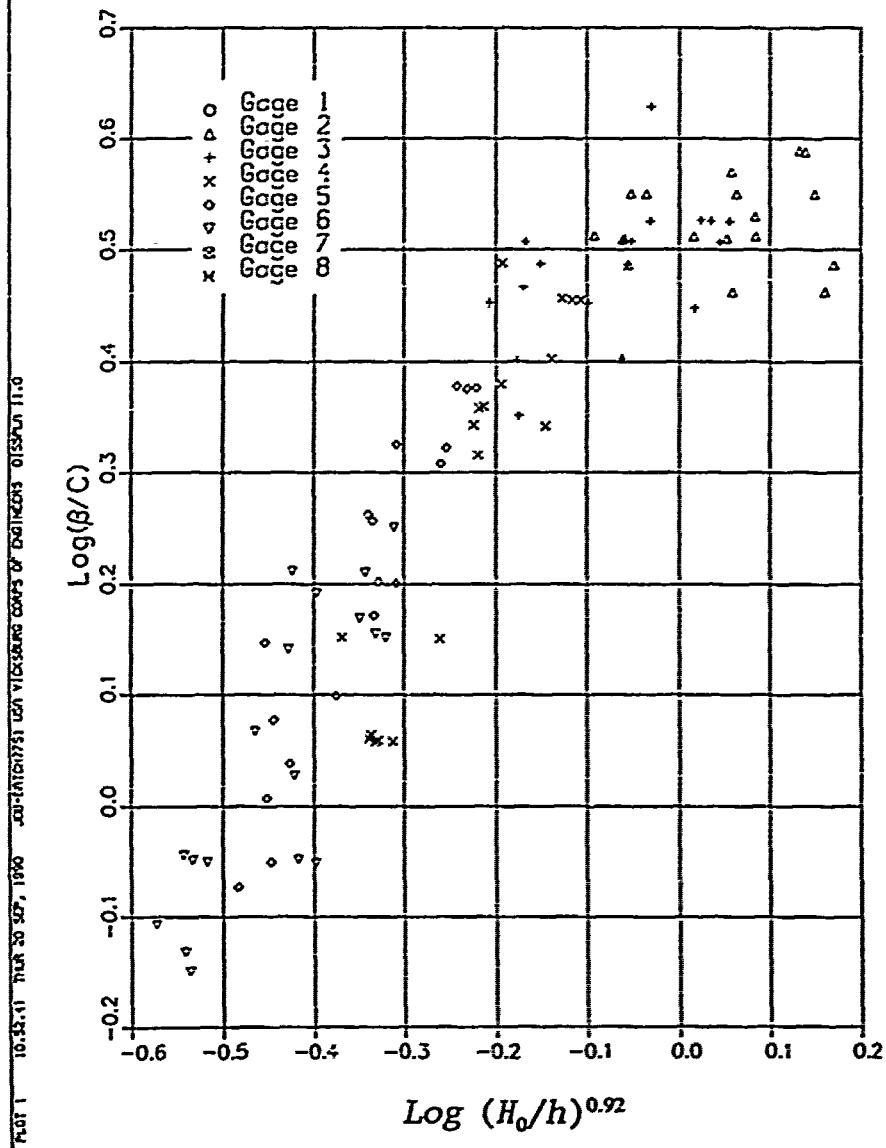


Figure 10. Modified regression results for B/C based on the local deepwater wave characteristics

FRF Spectral Parameter Analysis Stations 2 to 6

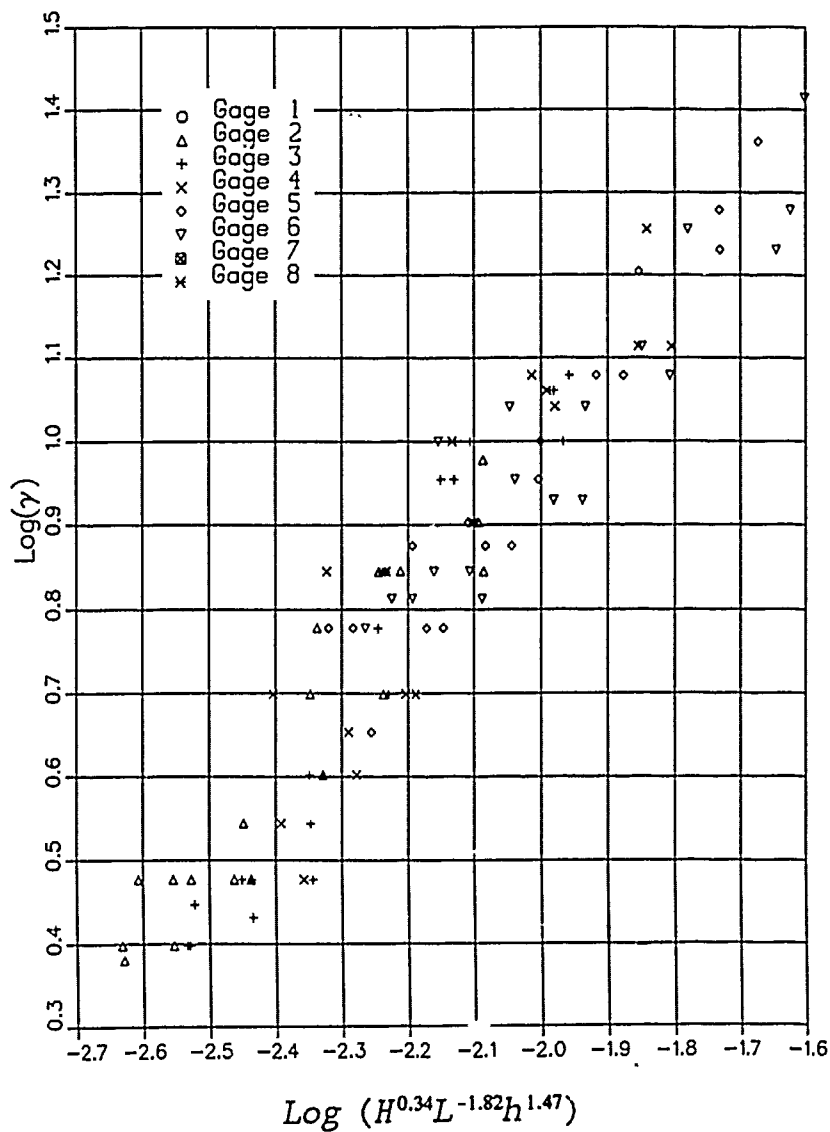


Figure 11. Regression results for γ based on local wave characteristics

FRF Spectral Parameter Analysis Stations 2 to 6

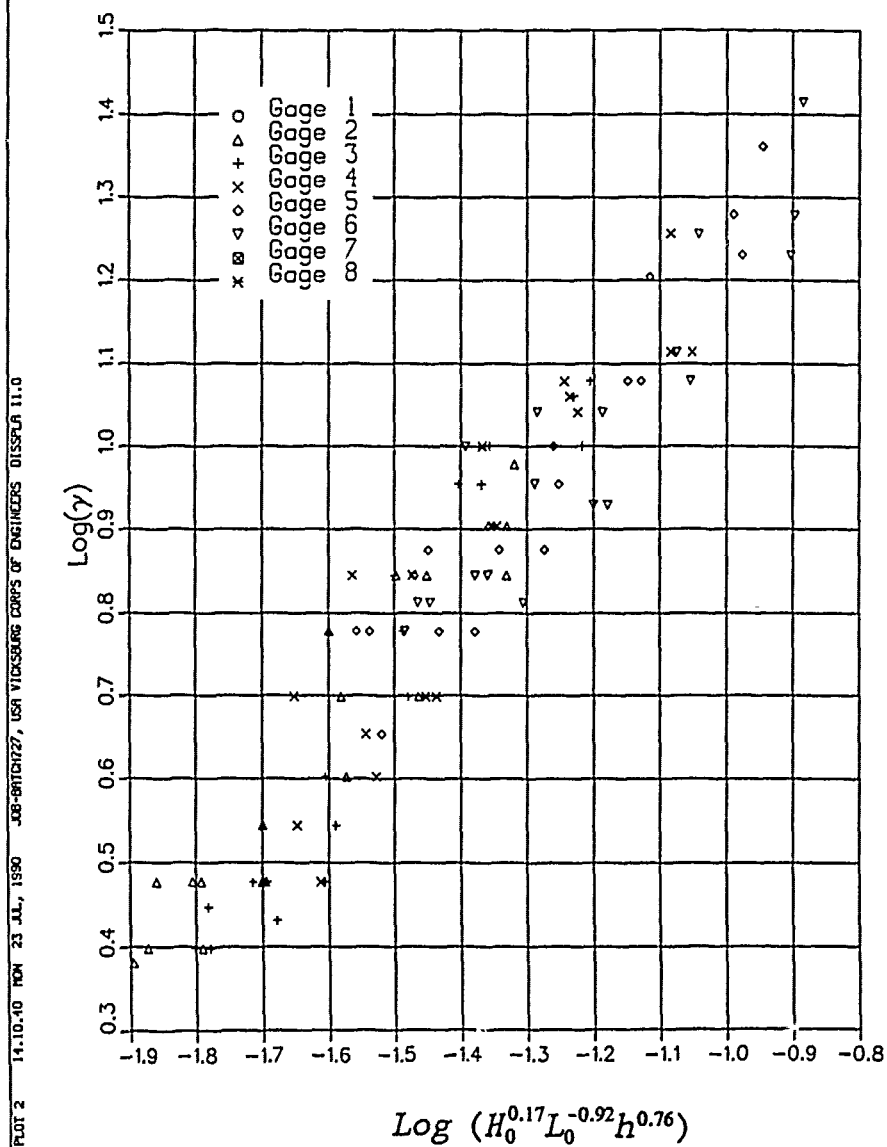


Figure 12. Regression results for γ based on the deepwater wave characteristics

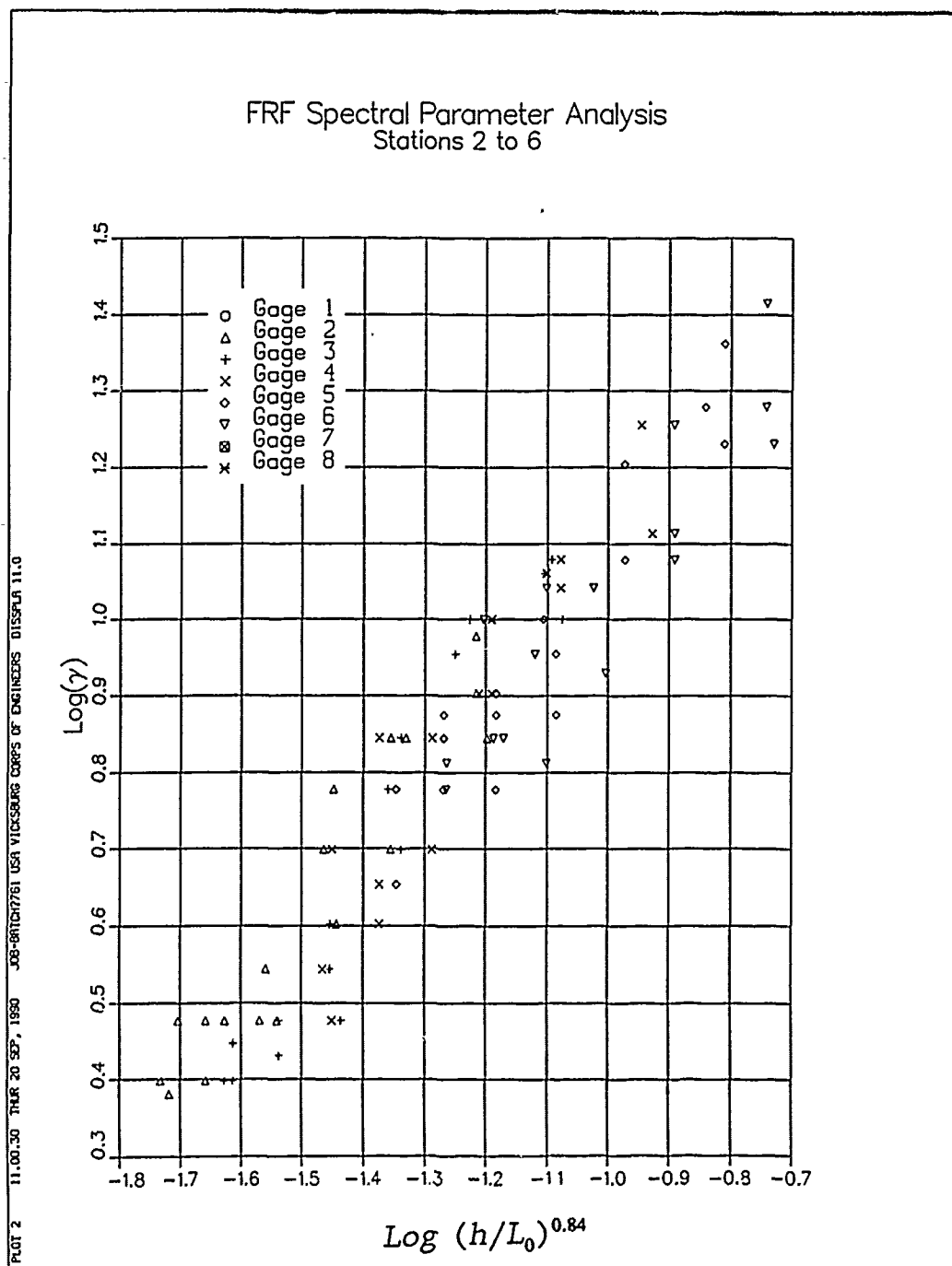


Figure 13. Modified regression results for γ based on the deepwater wave characteristics

Regression for σ_a and σ_b

22. The regression analyses for σ_a and σ_b indicated very little correlation between these parameters and the wave characteristics. The average value of σ_a in the surf zone was 0.11 with a standard deviation of 0.024, a variance of 0.001, a maximum value of 0.16, and a minimum value of 0.06. The average value of σ_b in the surf zone was 0.11 with a standard deviation of 0.031, a variance of 0.001, a maximum value of 0.19, and a minimum value of 0.04. As with γ , the average values for σ_a and σ_b must be applied with caution since the spectra generated in all of the laboratory tests had the same initial values for these parameters.

PART IV: APPLICATION IN SPECTRAL MODEL

23. The equational representations of the FRF spectral parameters discussed previously were implemented in the time-independent spectral model, STWAVE, which was then used to simulate the laboratory experiments. The results of the simulations show that the equational representations of the FRF spectral parameters reasonably approximate the laboratory data. The simulations do not verify that the equational representations are applicable to any other wave conditions or bathymetric geometries. Additional data sets must be acquired and simulated before such a verification is possible.

24. Prior to implementing the equational representations of the FRF spectral parameters in STWAVE, a criterion for determining when breaking occurs was defined. The laboratory data were evaluated to determine a reasonable criteria for breaking, at least for the laboratory data. Equation 22 was found to describe the data at breaking.

$$\frac{H}{h} = 0.243 \left(\frac{h}{gT^2} \right)^{-0.18} \quad (22)$$

Equation 22 and the laboratory data are plotted in Figure 14.

25. Equation 22 was used in STWAVE for determining when the limiting form of the FRF spectrum should be applied. The excess energy removed by limiting was equated to the energy lost during breaking.

26. The calculated spectra from STWAVE are compared with the measured laboratory spectra in Figures 15 through 23 for peak spectral periods of 1.5, 2.0, and 2.5 sec, and for wave heights of 0.03, 0.09, and 0.15 m.

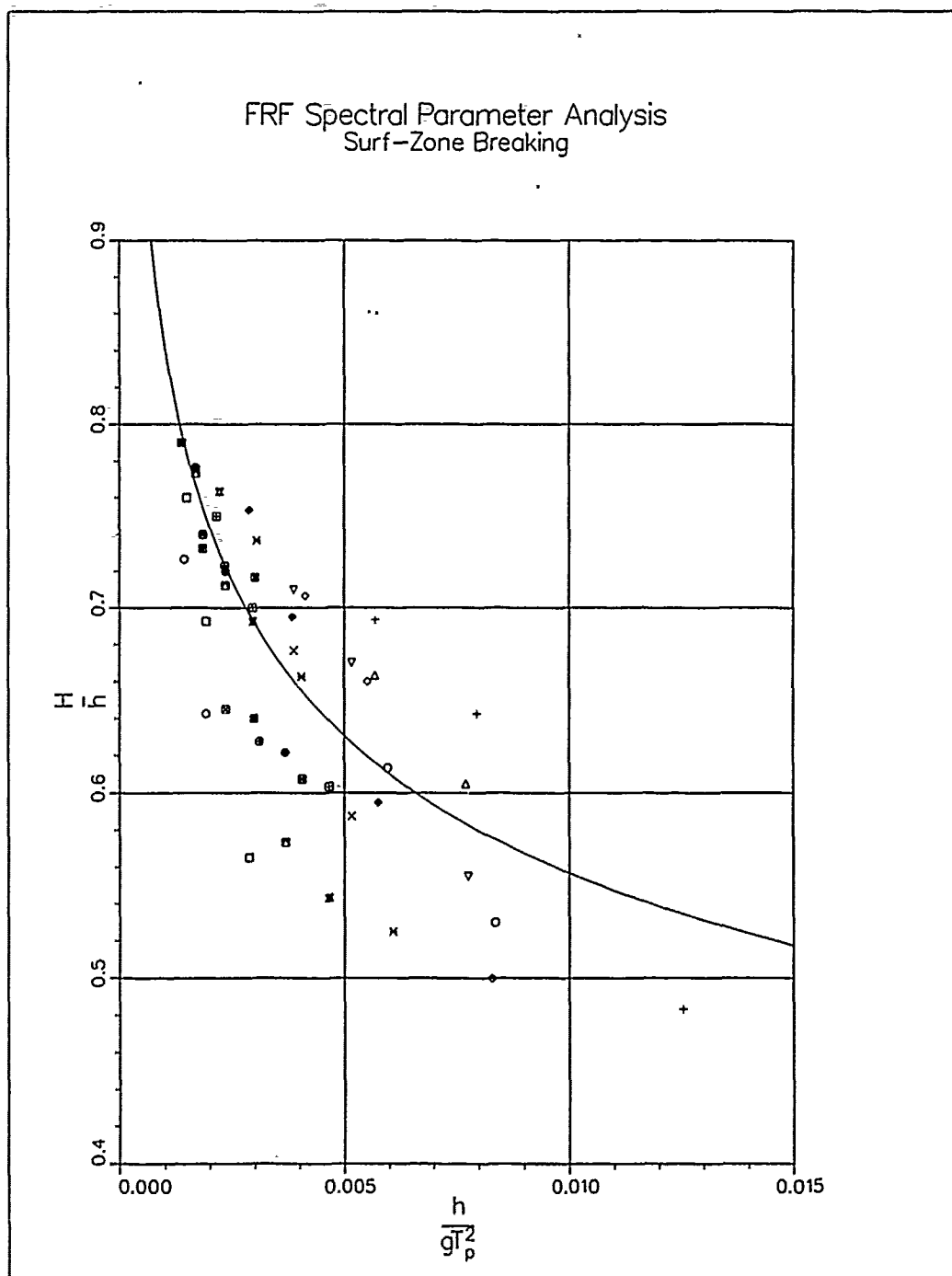
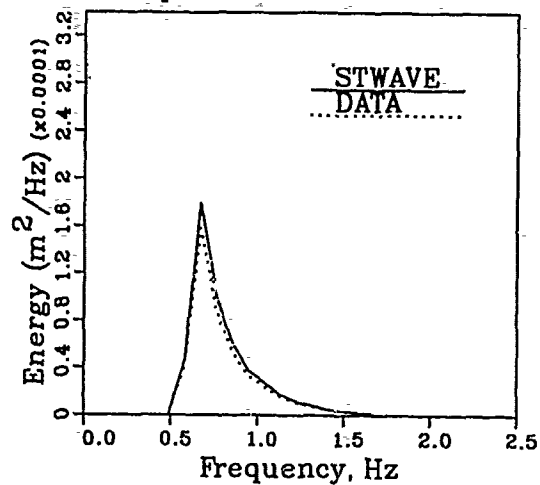


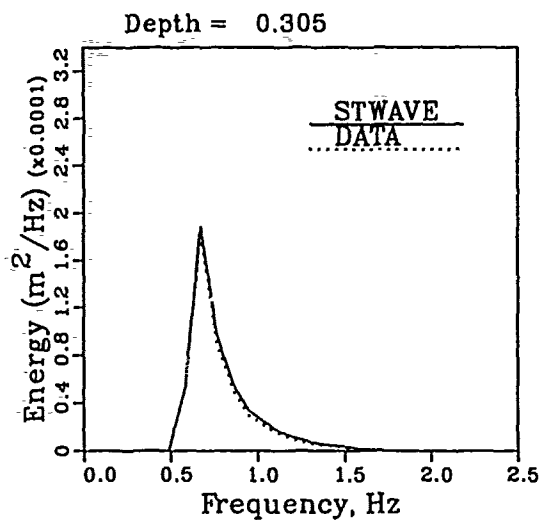
Figure 14. Breaking criteria

$T_p = 1.5s, H_n = 0.03m$

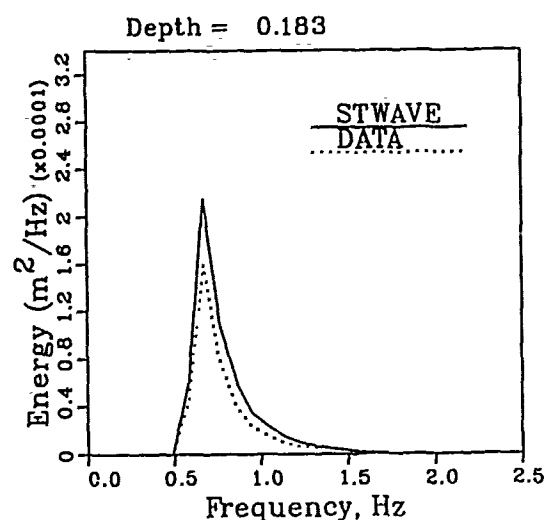
Depth = 0.609



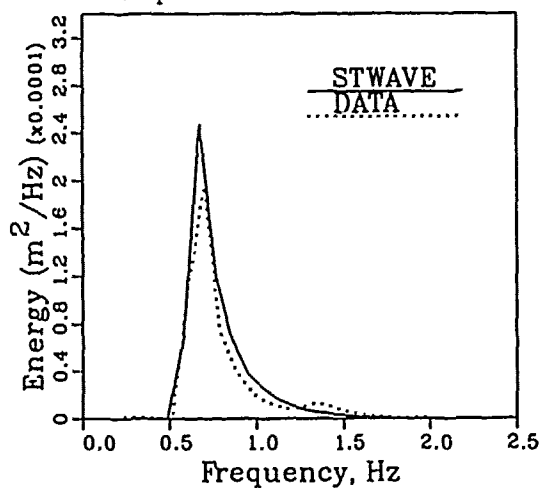
a. Depth = 0.609 m



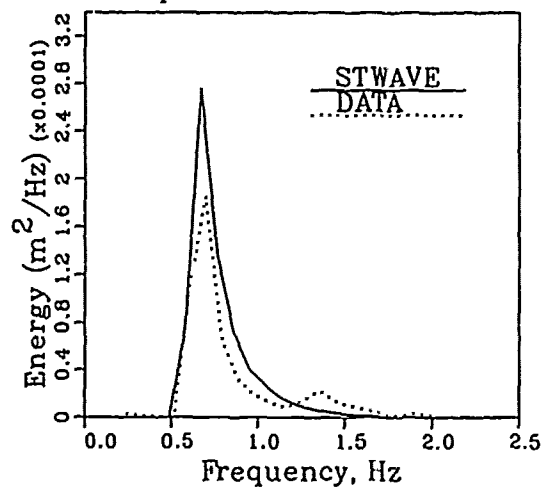
b. Depth = 0.305 m



c. Depth = 0.183 m



d. Depth = 0.122 m

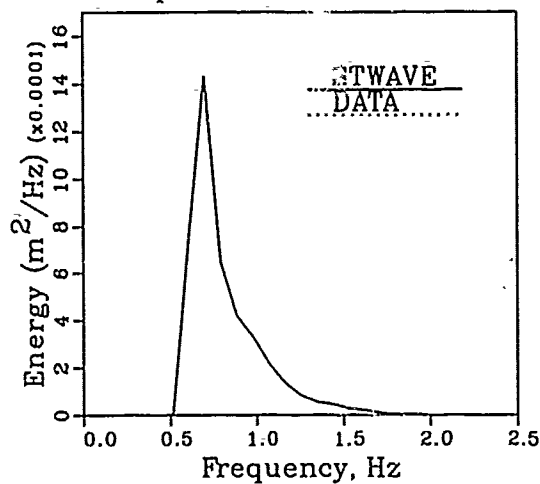


e. Depth = 0.091 m

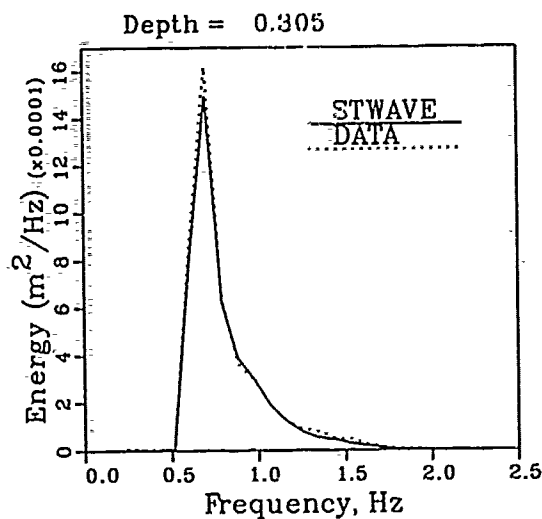
Figure 15. Comparisons of measured laboratory spectra with computed spectra from STWAVE, $T_p = 1.5$ sec, $H_n = 0.03$ m

$T_p = 1.5s, H_n = 0.09m$

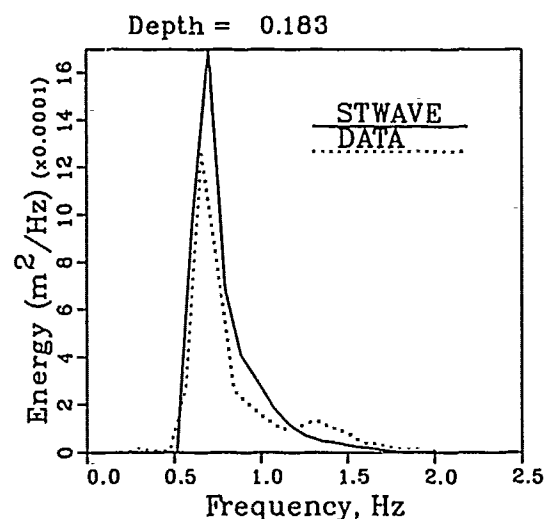
Depth = 0.609



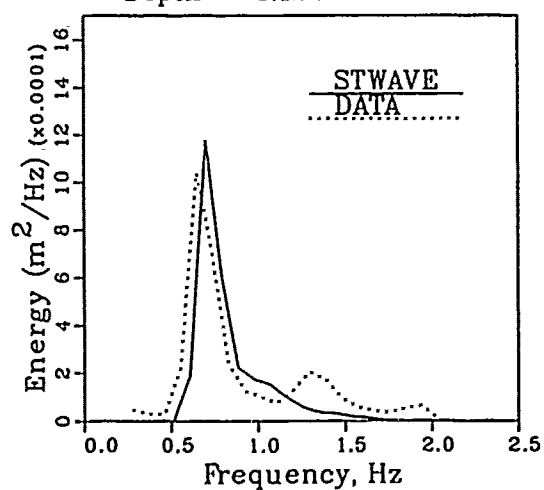
a. Depth = 0.609 m



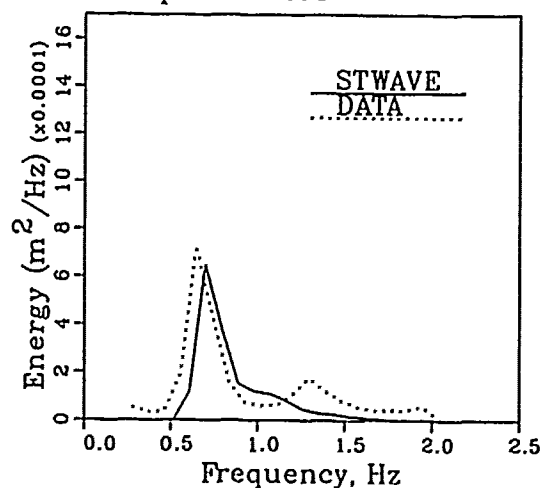
b. Depth = 0.305 m



c. Depth = 0.183 m



d. Depth = 0.122 m

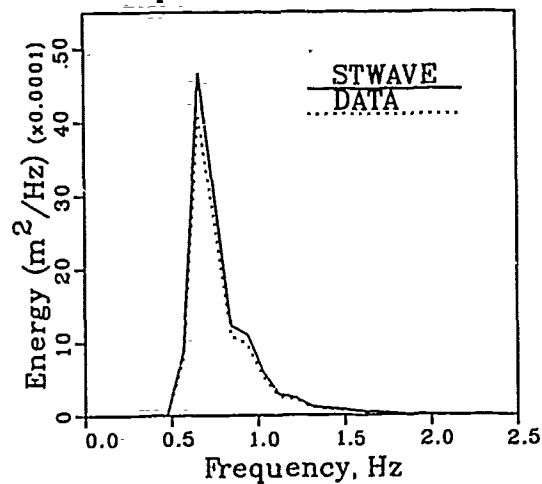


e. Depth = 0.091 m

Figure 16. Comparisons of measured laboratory spectra with computed spectra from STWAVE, $T_p = 1.5$ sec, $H_n = 0.09$ m

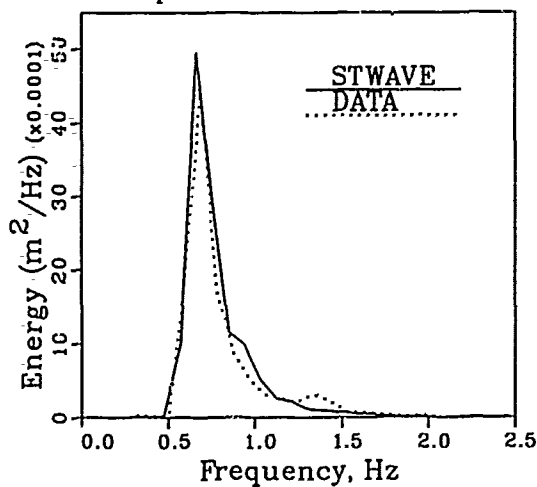
$T_p = 1.5s, H_n = 0.15m$

Depth = 0.609



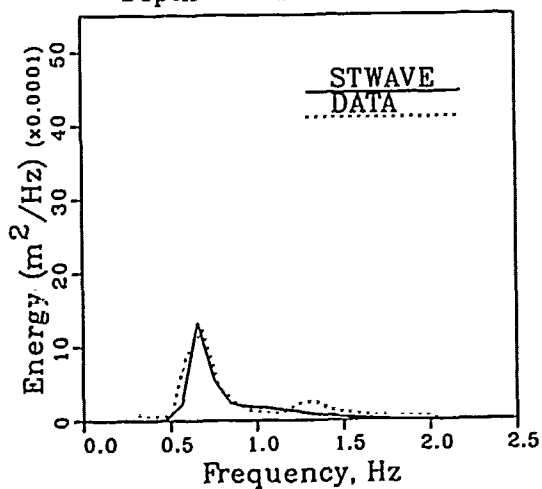
a. Depth = 0.609 m

Depth = 0.305



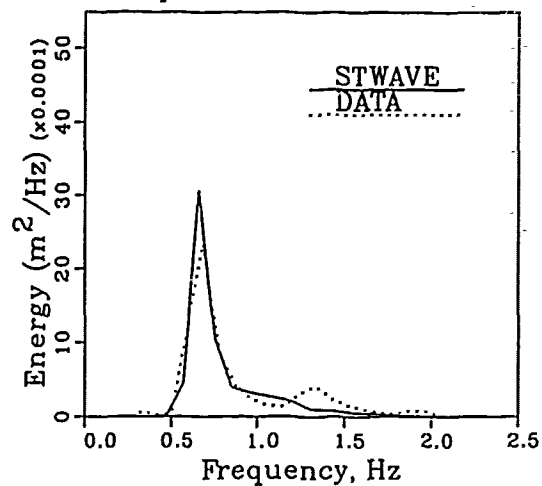
b. Depth = 0.305 m

Depth = 0.122



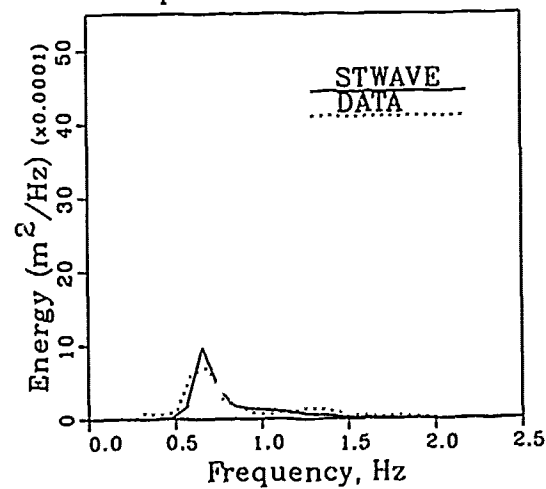
d. Depth = 0.122 m

Depth = 0.183



c. Depth = 0.183 m

Depth = 0.091

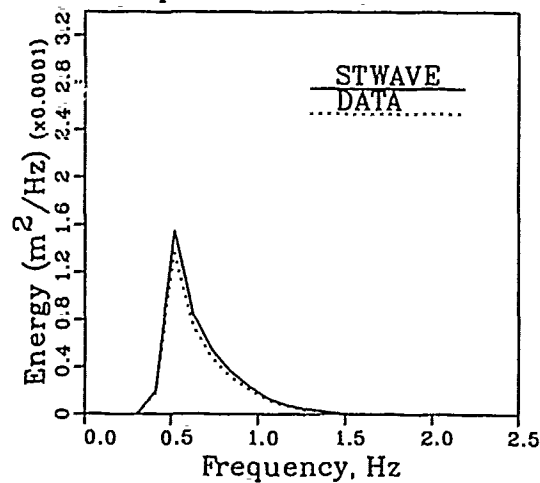


e. Depth = 0.091 m

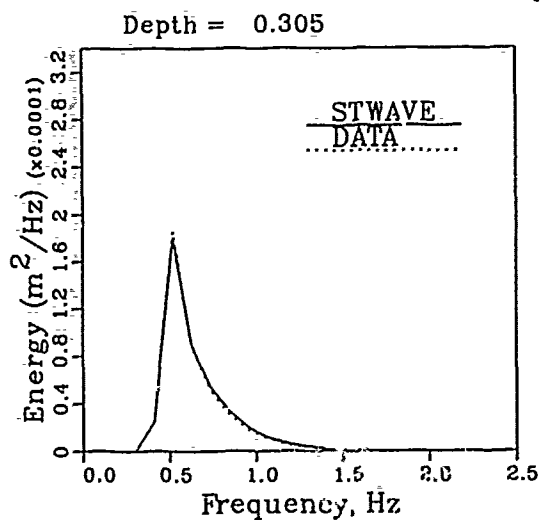
Figure 17. Comparisons of measured laboratory spectra with computed spectra from STWAVE, $T_p = 1.5$ sec, $H_n = 0.15$ m

$T_p = 2.0s, H_n = 0.03m$

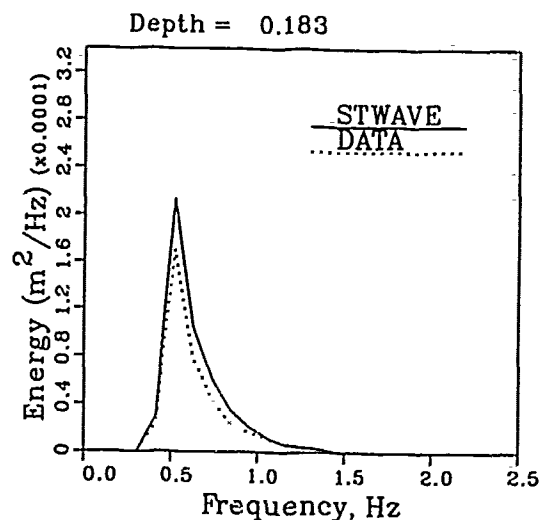
Depth = 0.609



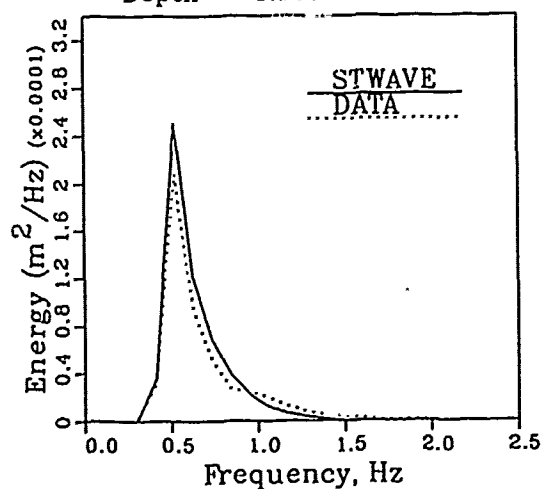
a. Depth = 0.609 m



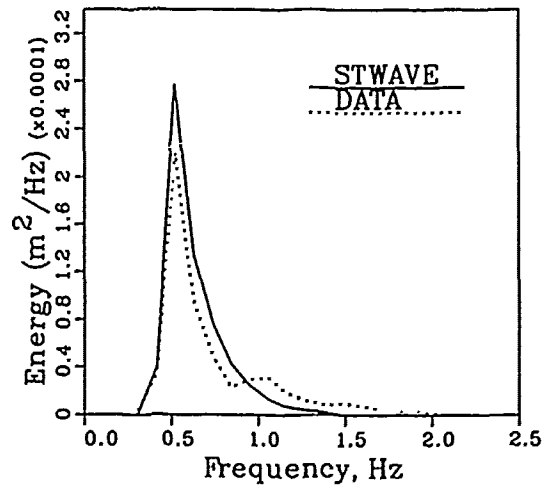
b. Depth = 0.305 m



c. Depth = 0.133 m



d. Depth = 0.122 m

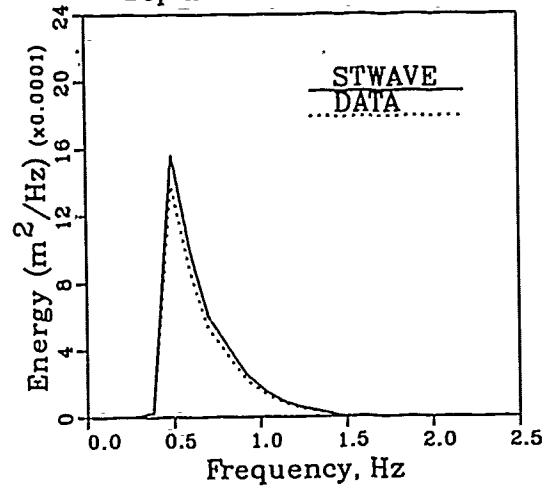


e. Depth = 0.091 m

Figure 18. Comparisons of measured laboratory spectra with computed spectra from STWAVE, $T_p = 2.0$ sec, $H_n = 0.03$ m

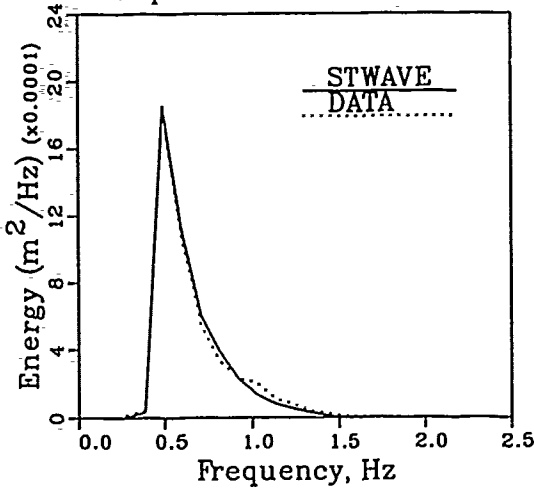
$T_p = 2.0s, H_n = 0.09m$

Depth = 0.609



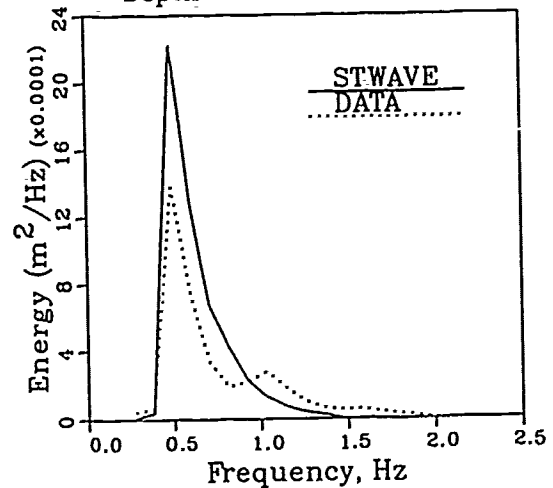
a. Depth = 0.609 m

Depth = 0.305



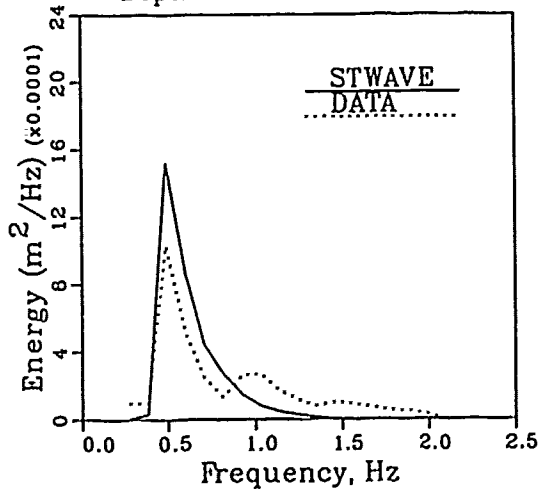
b. Depth = 0.305 m

Depth = 0.183



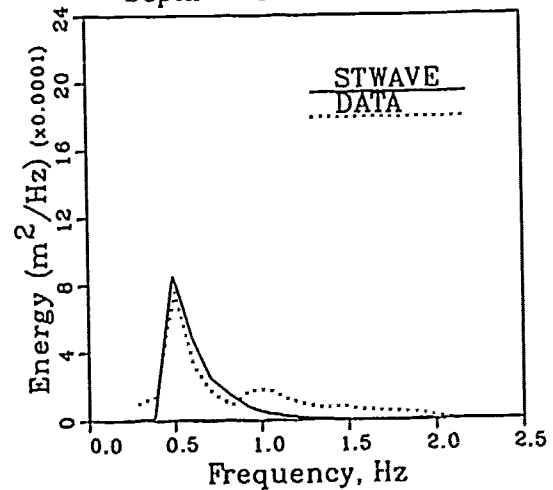
c. Depth = 0.183 m

Depth = 0.122



d. Depth = 0.122 m

Depth = 0.091

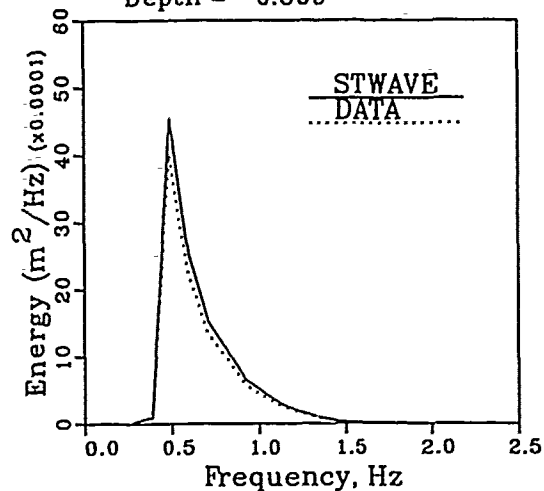


e. Depth = 0.091 m

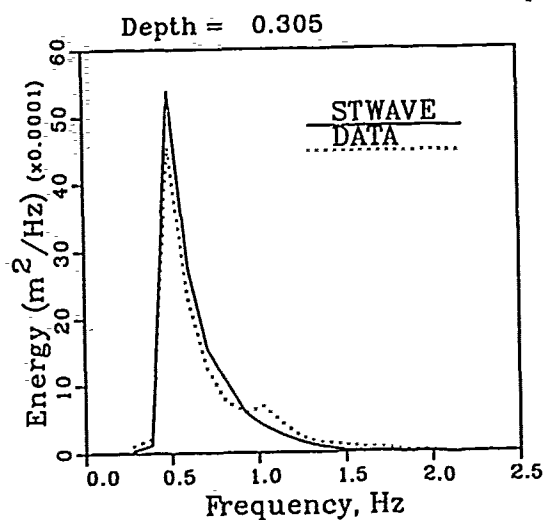
Figure 19. Comparisons of measured laboratory spectra with computed spectra from STWAVE, $T_p = 2.0$ sec, $H_n = 0.09$ m

$T_p = 2.0s, H_n = 0.15m$

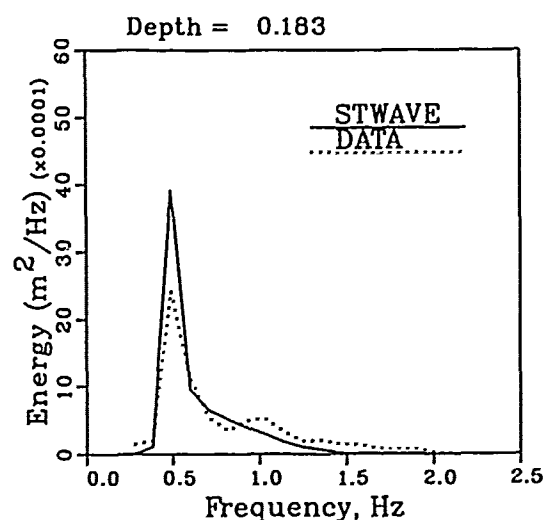
Depth = 0.609



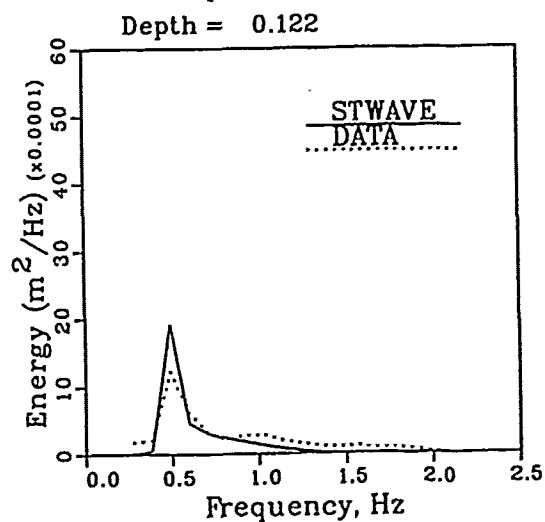
a. Depth = 0.609 m



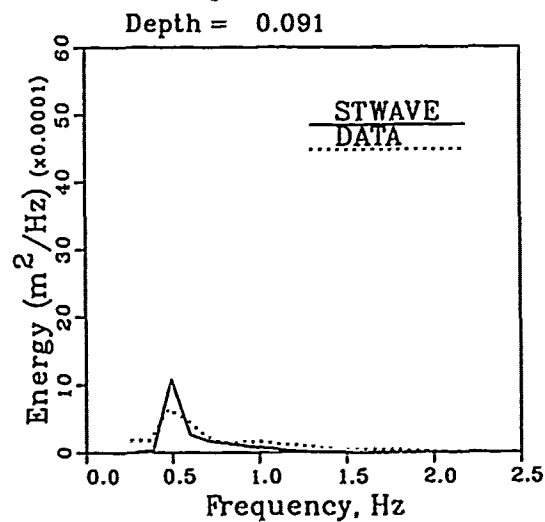
b. Depth = 0.305 m



c. Depth = 0.183 m



d. Depth = 0.122 m

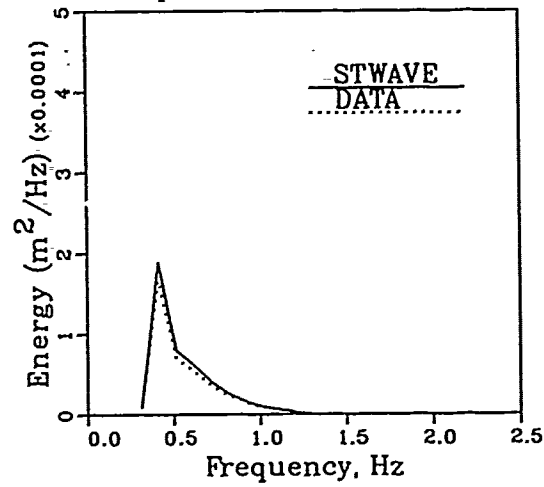


e. Depth = 0.091 m

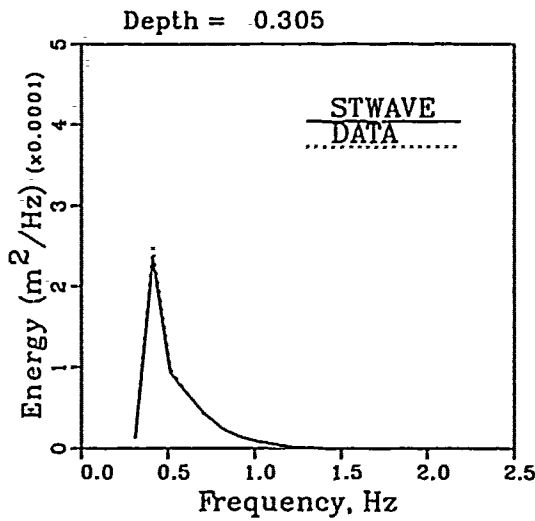
Figure 20. Comparisons of measured laboratory spectra with computed spectra from STWAVE, $T_p = 2.0$ sec, $H_n = 0.15$ m

$T_p = 2.5\text{s}$, $H_n = 0.03\text{m}$

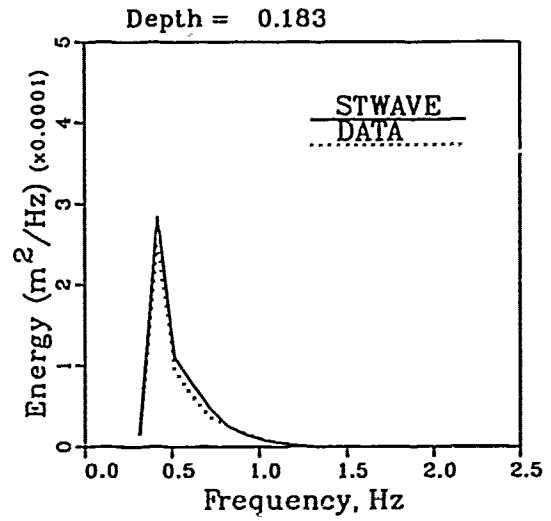
Depth = 0.609



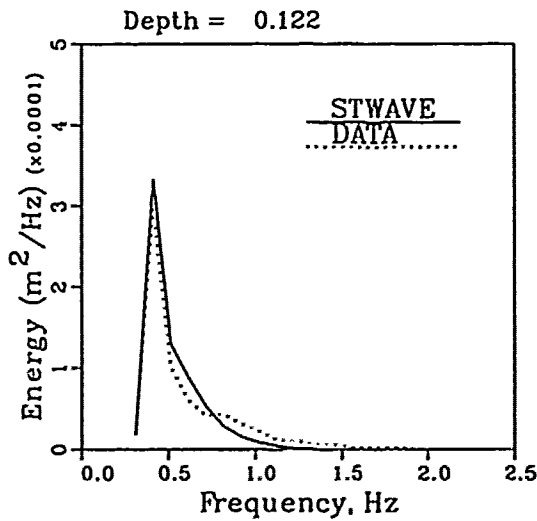
a. Depth = 0.609 m



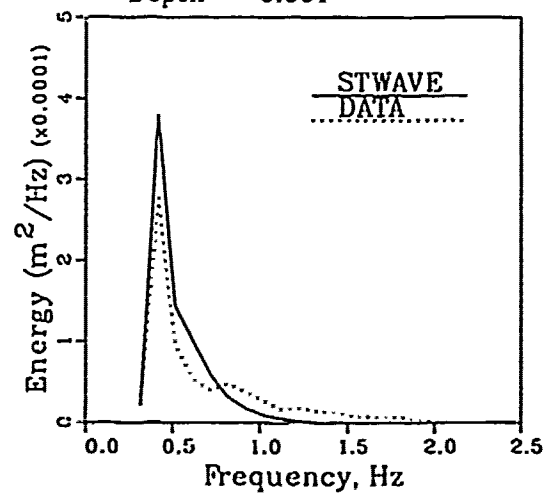
b. Depth = 0.305 m



c. Depth = 0.183 m



d. Depth = 0.122 m

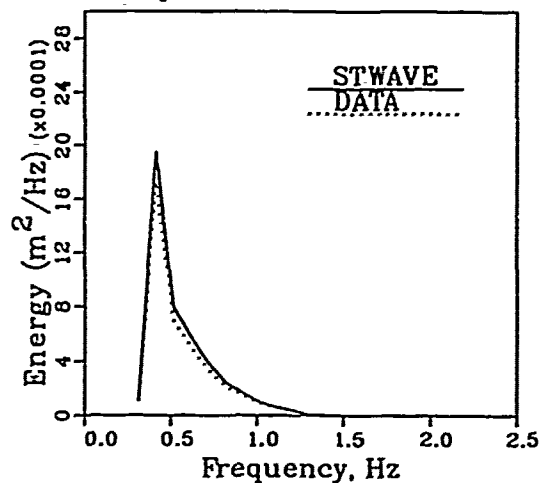


e. Depth = 0.091 m

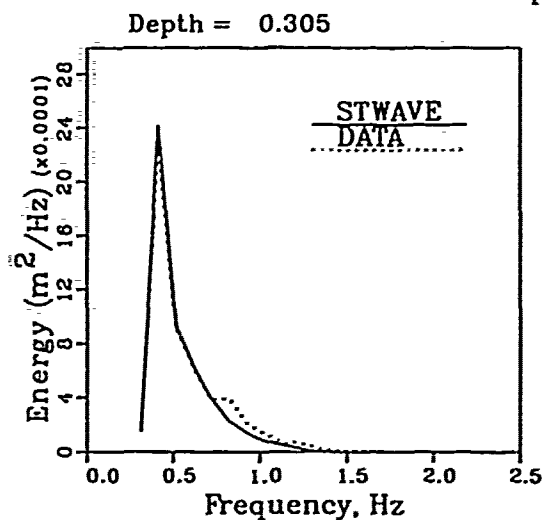
Figure 21. Comparisons of measured laboratory spectra with computed spectra from STWAVE, $T_p = 2.5\text{ sec}$, $H_n = 0.03\text{ m}$

$T_p = 2.5s, H_n = 0.09m$

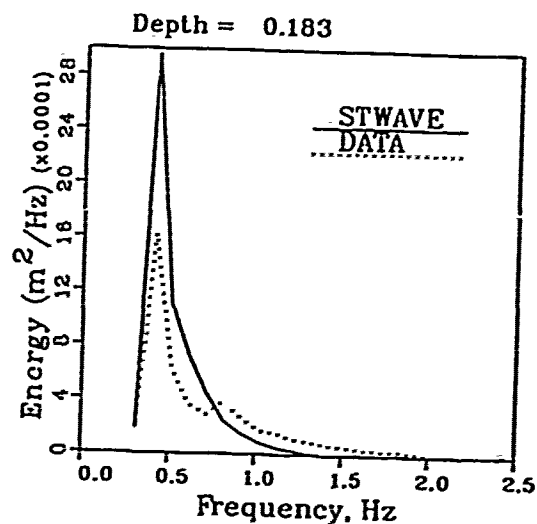
Depth = 0.609



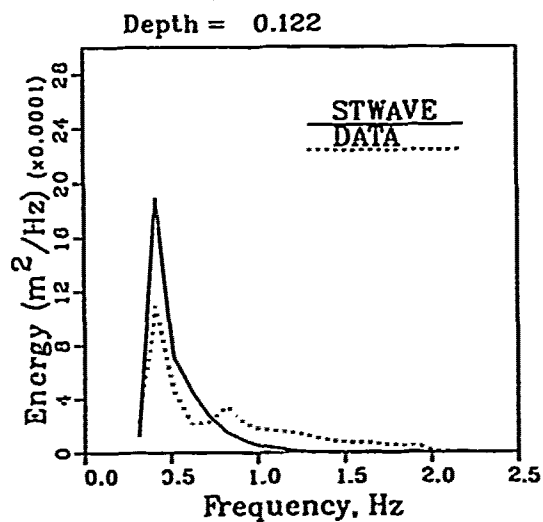
a. Depth = 0.609 m



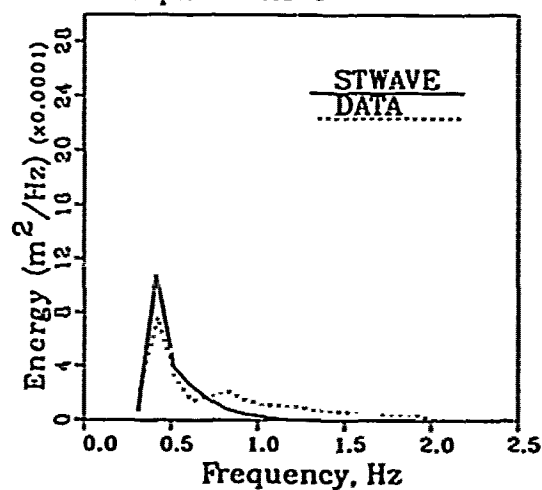
b. Depth = 0.305 m



c. Depth = 0.183 m



d. Depth = 0.122 m

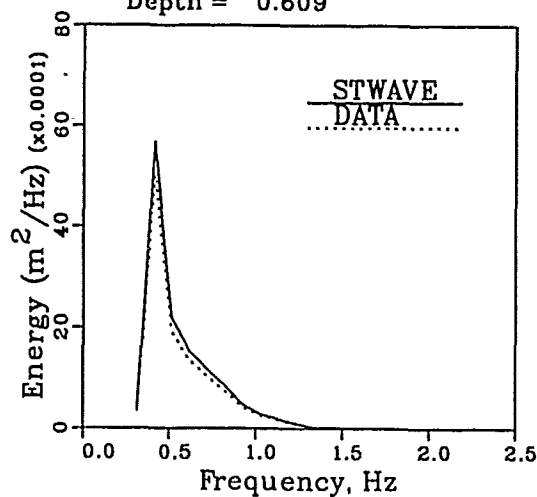


e. Depth = 0.091 m

Figure 22. Comparisons of measured laboratory spectra with computed spectra from STWAVE, $T_p = 2.5$ sec, $H_n = 0.09$ m

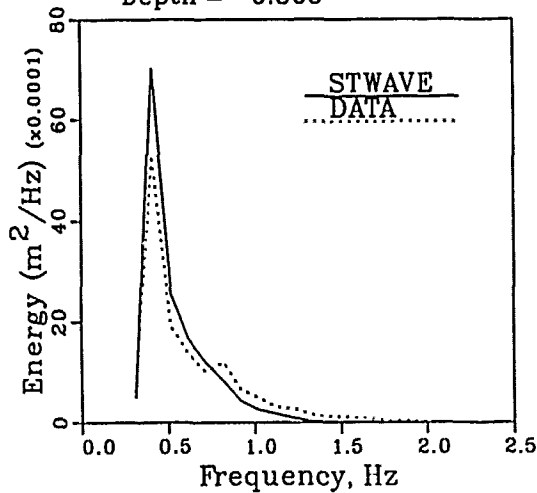
$T_p = 2.5\text{s}, H_n = 0.15\text{m}$

Depth = 0.609



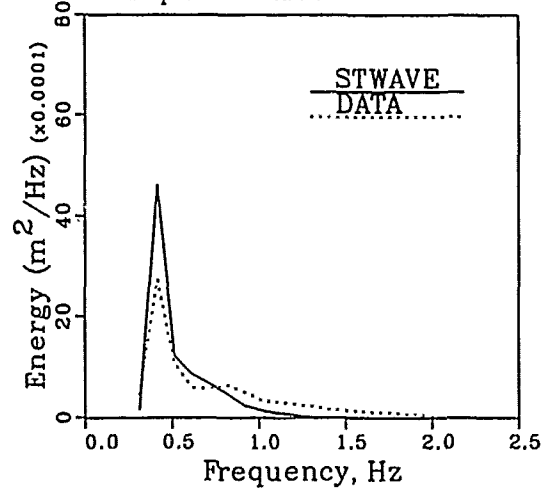
a. Depth = 0.609 m

Depth = 0.305



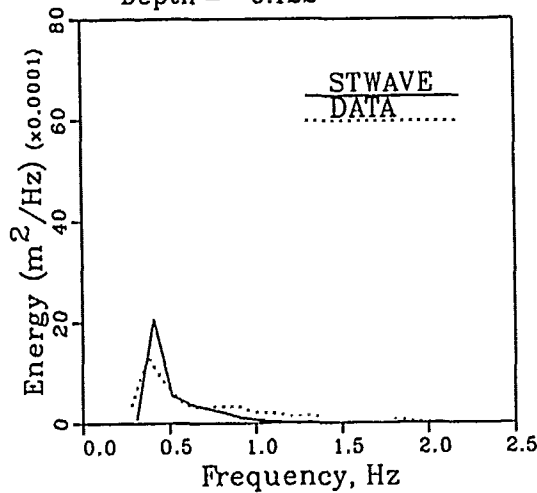
b. Depth = 0.305 m

Depth = 0.183



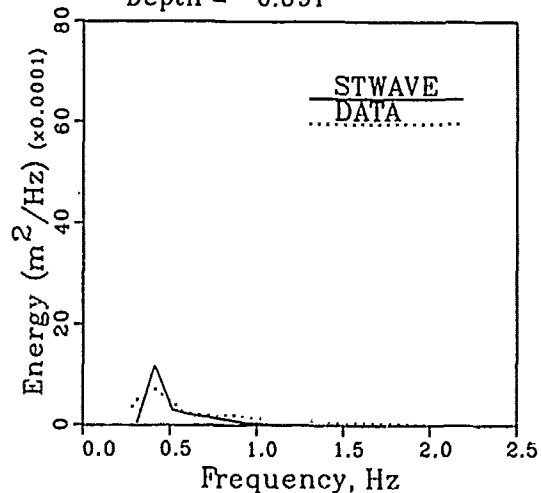
c. Depth = 0.183 m

Depth = 0.122



d. Depth = 0.122 m

Depth = 0.091



e. Depth = 0.091 m

Figure 23. Comparisons of measured laboratory spectra with computed spectra from STWAVE, $T_p = 2.5$ sec, $H_n = 0.15$ m

PART V: SUMMARY AND CONCLUSIONS

27. During the evaluation of laboratory experiments in which wave-energy spectra were propagated over a plane beach in a narrow flume, it was noted that the spectra transformed to a uniform spectral shape within the surf zone for a given peak spectral period, irrespective of the total spectral energy in deep water. Based on this observation, research was undertaken to determine means of describing the transformed wave-energy spectra within the surf zone. It was found that the FRF spectral description (Miller and Vincent 1990) could be used to describe the spectral shape with appropriate representation of the spectral parameters $(\beta/C, \gamma, \sigma_a, \sigma_b)$. Such representations were found for the given laboratory data by determining the values for the spectral parameters, such that the computed FRF spectrum fit the given measured spectrum. The values of the spectral parameters found for each of the laboratory spectra were then linearly regressed against selected nondimensional wave parameters. The recommended equational representation for γ is given by Equation 21. Average values are recommended for β/C , σ_a , or σ_b .

28. The analytical forms of β/C , γ , σ_a , and σ_b for the surf zone were implemented in the time-independent spectral wave model, STWAVE, to simulate the laboratory tests. The comparison is shown in Figure 15. It is concluded that wave spectra may be described through the surf zone in parametric form.

29. The parameter equations presented herein were based on a limited number of spectra, all of which had the same initial γ , σ_a , and σ_b values. The variability of these parameters for different sea states in a prototype environment was not modeled with these laboratory data. The transformation of true coastal spectra with directional spread over an irregular bottom should be simulated in the laboratory at least with similar conditions. With equivalent environmental and topographic conditions and careful analysis of measurements, it will be possible to better estimate nearshore wave climates from offshore measurements.

REFERENCES

Battjes, J. A. 1972. "Set-Up Due to Irregular Waves," Proceedings of the 13th International Conference on Coastal Engineering, American Society of Civil Engineers, pp 1993-2004.

Bouws, E., Günther, H., Rosenthal, W., and Vincent, C. L. 1985. "Similarity of the Wind Wave Spectrum in Finite Depth Water, Part I - Spectral Form," Journal of Geophysical Research, Vol 90, C1, pp 975-986.

Kitaigorodskii S. A. 1983. "On the Theory of the Equilibrium Range in the Spectrum of Wind-Generated Gravity Waves," Journal of Physical Oceanography, Vol 13, pp 816-827.

Miller, H. C., and Vincent, C. L. 1990. "FRF Spectrum: TMA with Kitaigorodskii's f^4 Scaling," Journal of Waterway, Port, Coastal, and Ocean Engineering, Vol 116, No. 1, pp 57-78.

Shore Protection Manual. 1984. 4th Ed., 2 Vol, US Army Engineer Waterways Experiment Station, Coastal Engineering Research Center, US Government Printing Office, Washington, DC.

APPENDIX A: WAVE CHARACTERISTIC AND FIELD RESEARCH FACILITY
SPECTRAL PARAMETER VALUES

GAGE	h	T _n	H _n	β	γ	σ_a	σ_b	H	T _p	L	L _o	H _o
1	0.061	1.25	0.091	4.57	5.0	0.16	0.13	0.054	1.25	0.96	2.44	0.073
1	0.061	1.25	0.122	4.57	5.5	0.11	0.11	0.056	1.28	0.99	2.56	0.095
1	0.061	1.25	0.152	4.57	5.5	0.11	0.11	0.057	1.28	0.99	2.56	0.113
1	0.061	1.50	0.091	4.57	4.5	0.10	0.08	0.058	1.55	1.20	3.75	0.079
1	0.061	1.50	0.122	3.96	4.0	0.09	0.12	0.060	1.58	1.22	3.90	0.104
1	0.061	1.50	0.152	3.96	4.0	0.10	0.10	0.059	1.58	1.22	3.90	0.127
1	0.061	1.75	0.091	4.11	4.0	0.13	0.06	0.060	1.75	1.35	4.78	0.078
1	0.061	1.75	0.122	4.11	2.5	0.13	0.11	0.061	1.85	1.43	5.34	0.105
1	0.061	1.75	0.152	3.99	2.8	0.14	0.11	0.063	1.85	1.43	5.34	0.129
1	0.061	2.00	0.091	3.81	2.8	0.14	0.09	0.063	2.05	1.58	6.56	0.080
1	0.061	2.00	0.122	3.66	2.8	0.28	0.09	0.065	2.05	1.58	6.56	0.107
1	0.061	2.00	0.152	3.35	3.0	0.10	0.06	0.063	2.10	1.62	6.88	0.133
1	0.061	2.25	0.091	3.66	3.0	0.13	0.06	0.065	2.28	1.76	8.11	0.084
1	0.061	2.25	0.122	3.66	3.0	0.25	0.06	0.069	2.28	1.76	8.11	0.112
1	0.061	2.25	0.152	3.05	2.8	0.28	0.06	0.068	2.33	1.80	8.47	0.140
1	0.061	2.50	0.091	3.05	2.3	0.11	0.07	0.063	2.58	1.99	10.39	0.080
1	0.061	2.50	0.122	3.05	2.5	0.08	0.08	0.066	2.60	2.01	10.55	0.106
1	0.061	2.50	0.152	2.90	2.0	0.10	0.08	0.068	2.65	2.05	10.96	0.137
2	0.091	1.25	0.091	3.05	7.0	0.13	0.14	0.056	1.25	1.17	2.44	0.073
2	0.091	1.25	0.122	3.05	8.0	0.10	0.14	0.061	1.28	1.20	2.56	0.095
2	0.091	1.25	0.152	3.05	9.5	0.10	0.14	0.063	1.28	1.20	2.56	0.113
2	0.091	1.50	0.091	3.05	7.0	0.09	0.10	0.062	1.55	1.46	3.75	0.079
2	0.091	1.50	0.122	3.05	7.0	0.15	0.10	0.065	1.50	1.41	3.51	0.104
2	0.091	1.50	0.152	3.66	5.0	0.12	0.10	0.065	1.55	1.46	3.75	0.127
2	0.091	1.75	0.091	3.05	6.0	0.09	0.07	0.066	1.76	1.66	4.83	0.078
2	0.091	1.75	0.122	3.51	4.0	0.16	0.11	0.067	1.75	1.65	4.78	0.105
2	0.091	1.75	0.152	3.66	5.0	0.10	0.09	0.069	1.80	1.70	5.06	0.129
2	0.091	2.00	0.091	3.35	3.0	0.13	0.08	0.066	2.00	1.89	6.24	0.080
2	0.091	2.00	0.122	3.35	3.5	0.12	0.09	0.070	2.05	1.94	6.56	0.107
2	0.091	2.00	0.152	3.35	3.0	0.08	0.08	0.069	2.08	1.97	6.75	0.133
2	0.091	2.25	0.091	3.35	3.0	0.10	0.05	0.068	2.25	2.13	7.90	0.084
2	0.091	2.25	0.122	3.20	3.0	0.09	0.08	0.071	2.35	2.22	8.62	0.112
2	0.091	2.25	0.152	2.90	2.5	0.16	0.10	0.071	2.35	2.22	8.62	0.140
2	0.091	2.50	0.091	2.90	2.4	0.09	0.06	0.066	2.55	2.41	10.15	0.080
2	0.091	2.50	0.122	2.74	3.0	0.14	0.06	0.069	2.50	2.37	9.75	0.106
2	0.091	2.50	0.152	2.74	2.5	0.10	0.08	0.072	2.60	2.46	10.55	0.137

(Continued)

(Sheet 1 of 4)

(Continued)

GAGE	h	T _n	H _n	β	γ	σ_s	σ_b	H	T _p	L	L _o	H _o
3	0.122	1.25	0.091	3.05	10.0	0.13	0.12	0.065	1.22	1.31	2.32	0.073
3	0.122	1.25	0.122	3.05	11.5	0.10	0.15	0.074	1.27	1.37	2.52	0.095
3	0.122	1.25	0.152	4.57	12.0	0.10	0.10	0.078	1.25	1.34	2.44	0.113
3	0.122	1.50	0.091	2.44	9.0	0.10	0.13	0.072	1.55	1.68	3.75	0.079
3	0.122	1.50	0.122	2.74	10.0	0.16	0.12	0.080	1.50	1.63	3.51	0.104
3	0.122	1.50	0.152	3.05	9.0	0.10	0.12	0.082	1.55	1.68	3.75	0.127
3	0.122	1.75	0.091	2.74	7.0	0.10	0.09	0.074	1.75	1.91	4.78	0.078
3	0.122	1.75	0.122	3.51	5.0	0.14	0.11	0.081	1.75	1.91	4.78	0.105
3	0.122	1.75	0.152	3.66	6.0	0.10	0.11	0.085	1.80	1.96	5.06	0.129
3	0.122	2.00	0.091	3.51	3.0	0.14	0.10	0.077	2.00	2.18	6.24	0.080
3	0.122	2.00	0.122	3.51	4.0	0.10	0.10	0.084	2.05	2.24	6.56	0.107
3	0.122	2.00	0.152	3.66	3.5	0.10	0.10	0.085	2.05	2.24	6.56	0.133
3	0.122	2.25	0.091	3.35	3.0	0.07	0.07	0.079	2.30	2.51	8.26	0.084
3	0.122	2.25	0.122	3.66	3.0	0.10	0.08	0.087	2.30	2.51	8.26	0.112
3	0.122	2.25	0.152	3.66	2.7	0.15	0.10	0.088	2.30	2.51	8.26	0.140
3	0.122	2.50	0.091	3.20	2.5	0.06	0.06	0.078	2.55	2.79	10.15	0.080
3	0.122	2.50	0.122	3.35	2.8	0.10	0.04	0.084	2.55	2.79	10.15	0.106
3	0.122	2.50	0.152	3.51	2.5	0.08	0.09	0.089	2.60	2.84	10.55	0.137
4	0.183	1.25	0.091	1.83	13.0	0.11	0.15	0.063	1.22	1.57	2.32	0.073
4	0.183	1.25	0.122	1.83	18.0	0.11	0.19	0.080	1.25	1.62	2.44	0.095
4	0.183	1.25	0.152	3.96	13.0	0.14	0.08	0.088	1.22	1.57	2.32	0.113
4	0.183	1.50	0.091	1.52	12.0	0.14	0.15	0.073	1.50	1.97	3.51	0.079
4	0.183	1.50	0.122	2.90	11.0	0.12	0.12	0.091	1.50	1.97	3.51	0.104
4	0.183	1.50	0.152	2.90	11.5	0.11	0.15	0.101	1.55	2.04	3.75	0.127
4	0.183	1.75	0.091	1.52	10.0	0.12	0.14	0.077	1.75	2.32	4.78	0.078
4	0.183	1.75	0.122	2.74	8.0	0.12	0.14	0.096	1.75	2.32	4.78	0.105
4	0.183	1.75	0.152	3.35	8.0	0.08	0.15	0.109	1.80	2.39	5.06	0.129
4	0.183	2.00	0.091	1.52	7.0	0.14	0.16	0.081	2.00	2.66	6.24	0.080
4	0.183	2.00	0.122	3.05	5.0	0.14	0.12	0.099	2.00	2.66	6.24	0.107
4	0.183	2.00	0.152	3.81	5.0	0.14	0.11	0.110	2.00	2.66	6.24	0.133
4	0.183	2.25	0.091	1.52	7.0	0.12	0.12	0.084	2.25	3.00	7.90	0.084
4	0.183	2.25	0.122	3.20	4.5	0.12	0.08	0.105	2.25	3.00	7.90	0.112
4	0.183	2.25	0.152	3.81	4.0	0.14	0.10	0.114	2.25	3.00	7.90	0.140
4	0.183	2.50	0.091	1.52	5.0	0.12	0.12	0.086	2.50	3.34	9.75	0.080
4	0.183	2.50	0.122	3.05	3.5	0.08	0.08	0.103	2.55	3.41	10.15	0.106
4	0.183	2.50	0.152	3.81	3.0	0.12	0.10	0.117	2.50	3.34	9.75	0.137

(continued)

(Sheet 2 of 4)

(Continued)

GAGE	h	T _n	H _n	β	γ	σ_a	σ_b	H	T _p	L	L _a	H _a
5	0.244	1.25	0.091	1.22	17.0	0.16	0.16	0.070	1.20	1.73	2.25	0.073
5	0.244	1.25	0.122	1.83	19.0	0.10	0.20	0.091	1.25	1.82	2.44	0.095
5	0.244	1.25	0.152	3.05	23.0	0.17	0.08	0.104	1.20	1.73	2.25	0.113
5	0.244	1.50	0.091	1.52	12.0	0.13	0.15	0.081	1.50	2.25	3.51	0.079
5	0.244	1.50	0.122	2.74	12.0	0.12	0.14	0.106	1.50	2.25	3.51	0.104
5	0.244	1.50	0.152	3.05	16.0	0.14	0.14	0.124	1.50	2.25	3.51	0.127
5	0.244	1.75	0.091	2.13	7.5	0.10	0.12	0.084	1.75	2.66	4.78	0.078
5	0.244	1.75	0.122	2.74	9.0	0.12	0.14	0.110	1.75	2.66	4.78	0.105
5	0.244	1.75	0.152	3.20	10.0	0.09	0.18	0.131	1.80	2.74	5.06	0.129
5	0.244	2.00	0.091	1.83	6.0	0.12	0.16	0.089	2.00	3.06	6.24	0.080
5	0.244	2.00	0.122	2.44	8.0	0.12	0.14	0.114	2.00	3.06	6.24	0.107
5	0.244	2.00	0.152	3.66	7.5	0.12	0.13	0.136	2.00	3.06	6.24	0.133
5	0.244	2.25	0.091	1.68	7.0	0.10	0.12	0.094	2.25	3.46	7.90	0.084
5	0.244	2.25	0.122	2.44	7.5	0.12	0.12	0.123	2.25	3.46	7.90	0.112
5	0.244	2.25	0.152	3.66	6.0	0.14	0.12	0.144	2.25	3.46	7.90	0.140
5	0.244	2.50	0.091	1.37	6.0	0.12	0.13	0.093	2.50	3.85	9.75	0.080
5	0.244	2.50	0.122	2.29	6.0	0.12	0.10	0.119	2.50	3.85	9.75	0.106
5	0.244	2.50	0.152	3.66	4.5	0.12	0.12	0.144	2.50	3.85	9.75	0.137
6	0.305	1.25	0.091	1.22	17.0	0.13	0.16	0.072	1.20	1.87	2.25	0.073
6	0.305	1.25	0.122	1.83	19.0	0.12	0.16	0.094	1.22	1.91	2.32	0.095
6	0.305	1.25	0.152	2.44	26.0	0.12	0.10	0.109	1.22	1.91	2.32	0.113
6	0.305	1.50	0.091	1.22	13.0	0.12	0.14	0.081	1.50	2.48	3.51	0.079
6	0.305	1.50	0.122	2.29	12.0	0.13	0.14	0.108	1.50	2.48	3.51	0.104
6	0.305	1.50	0.152	2.44	18.0	0.14	0.14	0.129	1.50	2.48	3.51	0.127
6	0.305	1.75	0.091	1.52	8.5	0.10	0.14	0.084	1.75	2.95	4.78	0.078
6	0.305	1.75	0.122	2.74	8.5	0.10	0.14	0.112	1.75	2.95	4.78	0.105
6	0.305	1.75	0.152	2.74	11.0	0.09	0.18	0.136	1.80	3.04	5.06	0.129
6	0.305	2.00	0.091	1.52	6.5	0.12	0.14	0.089	2.00	3.40	6.24	0.080
6	0.305	2.00	0.122	1.52	11.0	0.14	0.17	0.117	2.00	3.40	6.24	0.107
6	0.305	2.00	0.152	2.44	9.0	0.10	0.18	0.141	2.05	3.49	6.56	0.133
6	0.305	2.25	0.091	1.52	7.0	0.12	0.10	0.093	2.20	3.76	7.55	0.084
6	0.305	2.25	0.122	1.52	10.0	0.08	0.16	0.124	2.30	3.94	8.26	0.112
6	0.305	2.25	0.152	3.05	7.0	0.12	0.12	0.150	2.25	3.85	7.90	0.140
6	0.305	2.50	0.091	1.22	6.0	0.11	0.12	0.093	2.50	4.29	9.75	0.080
6	0.305	2.50	0.122	1.83	6.5	0.12	0.12	0.121	2.50	4.29	9.75	0.106
6	0.305	2.50	0.152	2.44	6.5	0.12	0.14	0.149	2.50	4.29	9.75	0.137

(Continued)

(Sheet 3 of 4)

(Concluded)

GAGE	h	T _n	H _n	β	γ	σ_s	σ_b	H	T _p	L	L _o	H _o
7	0.457	1.25	0.091	1.22	11.5	0.12	0.15	0.069	1.20	2.08	2.25	0.073
7	0.457	1.25	0.122	1.37	15.5	0.12	0.20	0.090	1.22	2.13	2.32	0.095
7	0.457	1.25	0.152	2.44	16.0	0.12	0.12	0.106	1.22	2.13	2.32	0.113
7	0.457	1.50	0.091	1.52	6.5	0.10	0.12	0.076	1.50	2.88	3.51	0.079
7	0.457	1.50	0.122	2.44	7.2	0.10	0.13	0.101	1.50	2.88	3.51	0.104
7	0.457	1.50	0.152	3.05	9.2	0.12	0.13	0.123	1.50	2.88	3.51	0.127
7	0.457	1.75	0.091	1.22	6.0	0.10	0.12	0.075	1.75	3.50	4.78	0.078
7	0.457	1.75	0.122	1.83	8.0	0.11	0.11	0.101	1.75	3.50	4.78	0.105
7	0.457	1.75	0.152	2.59	8.0	0.10	0.12	0.124	1.77	3.55	4.89	0.129
7	0.457	2.00	0.091	0.91	6.2	0.12	0.14	0.078	2.00	4.09	6.24	0.080
7	0.457	2.00	0.122	1.83	6.0	0.09	0.13	0.104	2.00	4.09	6.24	0.107
7	0.457	2.00	0.152	2.44	6.0	0.10	0.15	0.130	2.05	4.21	6.56	0.133
7	0.457	2.25	0.091	0.91	6.0	0.10	0.10	0.080	2.25	4.66	7.90	0.084
7	0.457	2.25	0.122	1.68	5.5	0.10	0.10	0.109	2.25	4.66	7.90	0.112
7	0.457	2.25	0.152	2.44	6.0	0.10	0.12	0.136	2.25	4.66	7.90	0.140
7	0.457	2.50	0.091	0.61	7.0	0.10	0.12	0.080	2.50	5.22	9.75	0.080
7	0.457	2.50	0.122	1.22	6.0	0.10	0.12	0.107	2.50	5.21	9.75	0.106
7	0.457	2.50	0.152	2.13	5.5	0.10	0.12	0.135	2.50	5.21	9.75	0.137
8	0.610	1.25	0.091	1.22	10.0	0.12	0.15	0.073	1.20	2.17	2.25	0.073
8	0.610	1.25	0.122	1.07	21.0	0.14	0.18	0.095	1.20	2.17	2.25	0.095
8	0.610	1.25	0.152	1.37	25.0	0.12	0.15	0.113	1.22	2.24	2.32	0.113
8	0.610	1.50	0.091	0.91	9.0	0.12	0.15	0.079	1.50	3.14	3.51	0.079
8	0.610	1.50	0.122	1.22	12.0	0.12	0.16	0.104	1.50	3.14	3.51	0.104
8	0.610	1.50	0.152	1.83	13.0	0.12	0.16	0.127	1.50	3.14	3.51	0.127
8	0.610	1.75	0.091	1.07	6.0	0.10	0.12	0.078	1.75	3.90	4.78	0.078
8	0.610	1.75	0.122	1.98	6.5	0.12	0.10	0.105	1.70	3.75	4.51	0.105
8	0.610	1.75	0.152	1.83	10.5	0.10	0.13	0.129	1.75	3.90	4.78	0.129
8	0.610	2.00	0.091	0.70	6.2	0.10	0.15	0.080	2.00	4.62	6.24	0.080
8	0.610	2.00	0.122	1.83	4.5	0.07	0.12	0.107	2.00	4.62	6.24	0.107
8	0.610	2.00	0.152	2.53	5.2	0.10	0.12	0.133	2.00	4.75	6.24	0.133
8	0.610	2.25	0.091	0.76	5.5	0.10	0.12	0.084	2.25	5.30	7.90	0.084
8	0.610	2.25	0.122	1.52	4.8	0.10	0.12	0.112	2.25	5.30	7.90	0.112
8	0.610	2.25	0.152	2.29	5.2	0.10	0.12	0.140	2.25	5.30	7.90	0.140
8	0.610	2.50	0.091	0.61	5.2	0.10	0.12	0.080	2.50	5.96	9.75	0.080
8	0.610	2.50	0.122	1.13	5.0	0.10	0.12	0.106	2.50	5.96	9.75	0.106
8	0.610	2.50	0.152	1.68	5.5	0.10	0.14	0.137	2.50	5.96	9.75	0.137

(Sheet 4 of 4)